AD NUMBER

AD868290

LIMITATION CHANGES

TO:

Approved for public release; distribution is unlimited.

FROM:

Distribution authorized to U.S. Gov't. agencies and their contractors; Critical Technology; APR 1970. Other requests shall be referred to Air Force Arnold Engineering Development Center, Attn: AETS, Arnold AFB, TN 37389. This document contains export-controlled technical data.

AUTHORITY

aedc usaf ltr, 13 mar 1973

AEDC-TR-70-72

[redacted]

[redacted]

EVALUATION OF INTERFERENCE EFFECTS ON A LIFTING MODEL IN THE AEDC-PWT 4-FT TRANSONIC TUNNEL

J. L. Jacocks

ARO, Inc.

April 1970

This document has been approved for public release; its distribution is unlimited. Ltr dated 13 March 73 signed by L. O. Cole

PROPULSION WIND TUNNEL FACILITY
ARNOLD ENGINEERING DEVELOPMENT CENTER
AIR FORCE SYSTEMS COMMAND
ARNOLD AIR FORCE STATION, TENNESSEE

[redacted]

[redacted]

[redacted]

[redacted]

NOTICES

When U. S. Government drawings specifications, or other data are used for any purpose other than a definitely related Government procurement operation, the Government thereby incurs no responsibility nor any obligation whatsoever, and the fact that the Government may have formulated, furnished, or in any way supplied the said drawings, specifications, or other data, is not to be regarded by implication or otherwise, or in any manner licensing the holder or any other person or corporation, or conveying any rights or permission to manufacture, use, or sell any patented invention that may in any way be related thereto.

Qualified users may obtain copies of this report from the Defense Documentation Center.

References to named commercial products in this report are not to be considered in any sense as an endorsement of the product by the United States Air Force or the Government.

[redacted]

[redacted]

EVALUATION OF INTERFERENCE EFFECTS ON A LIFTING MODEL IN THE AEDC-PWT 4-FT TRANSONIC TUNNEL

J. L. Jacocks
ARO, Inc.

FOREWORD

The work reported herein was sponsored by Headquarters, Arnold Engineering Development Center (AEDC), Air Force Systems Command (AFSC), Arnold Air Force Station, Tennessee, under Program Element 65401F/06RB.

The results of research presented were obtained by ARO, Inc. (a subsidiary of Sverdrup & Parcel and Associates, Inc.), contract operator of AEDC, AFSC, under Contract F40600-69-C-0001. The test was conducted September 6, 1969, under ARO Project No. PC2993, and the manuscript was submitted for publication on February 11, 1970.

The author takes this opportunity to thank the General Dynamics Corporation, Fort Worth, for the loan of the model and balance, Mr. Gary Kaftan of General Dynamics, and Mr. Earl Price and Mr. W. E. Carleton of ARO, Inc., project engineers for the tests.

This technical report has been reviewed and approved.

George F. Garey
Lt Colonel, USAF
AF Representative, PWT
Directorate of Test

Roy R. Croy, Jr.
Colonel, USAF
Director of Test

ABSTRACT

Tests were conducted in the AEDC Aerodynamic Wind Tunnel (4T) to evaluate subsonic and supersonic wall interference effects and general data quality using a modified F-111A aircraft model of 0.6-percent blockage. The tunnel is equipped with inclined-hole, variable porosity test section walls. Comparisons of the data obtained in Tunnel 4T with data obtained in the Propulsion Wind Tunnel (16T) using the same model, balance, and sting show that practically interference-free data can be obtained in Tunnel 4T throughout the Mach number range from 0.7 to 1.2 utilizing variable porosity. At other than the optimum wall porosities, experimental subsonic lift interference effects are generally larger than theoretical predictions, although theory and experiment are in qualitative agreement.

CONTENTS

APPENDIXES

I. ILLUSTRATIONS

Figure

NOMENCLATURE

a	Lift slope, $dC_L/d\alpha$, per radian
b	Reference wing span, 22.524 in.
C	Tunnel 4T test section area, 16 ft^2
C_D	Forebody drag coefficient, $C_{D_m} - (C_{D_I} + C_{D_b} + 2\ C_{D_p})$
C_{D_b}	Fuselage base pressure drag coefficient
C_{D_I}	Internal drag coefficient

C_{D_m}	Measured drag coefficient, drag/$q_\infty S$
C_{D_p}	Plug base pressure drag coefficient
C_L	Lift coefficient, lift/$q_\infty S$
C_m	Pitching-moment coefficient, pitching moment/$q_\infty S\bar{c}$
$C_{m_{\alpha_t}}$	Tail effectiveness, $dC_m/d\alpha_t$, per radian
$\bar{c}$	Reference mean aerodynamic chord, 6.583 in.
h	Tunnel 4T test section half height, 24 in.
ℓ	Horizontal tail moment arm, 11.276 in.
M	Mach number
m	Pitching-moment slope, dC_m/dC_L
p	Pressure, psfa
q	Dynamic pressure, psf
S	Reference wing area, 0.8651 ft^2
S_t	Reference horizontal tail area, 0.2676 ft^2
α	Model wing angle of attack, deg
α_t	Model tail angle of attack, deg
β	Mach number function, $\left(1 - M_\infty^2\right)^{1/2}$
δ_0	Lift interference factor because of upwash
δ_1	Lift interference factor because of streamline curvature
λ	Tunnel pressure ratio, p_t/p_e
τ	Test section wall porosity, percent

SUBSCRIPTS

0	Zero lift condition
e	Diffuser exit condition
i	Interference free condition
t	Stagnation condition or horizontal tail
∞	Free-stream condition

SECTION I
INTRODUCTION

This investigation was conducted to document the quality of data obtained in the Aerodynamic Wind Tunnel (4T) at AEDC. Specific areas of interest were subsonic and supersonic wall interference effects, tunnel flow angularity, and the influence of deviations from standard tunnel operation procedures.

The model used for this study was a 1/24-scale F-111A with a special fixed-sweep wing. The various interference effects were isolated by comparing the data obtained in Tunnel 4T with data obtained in the Propulsion Wind Tunnel (16T) using the identical model, balance, and sting. The tests were conducted at a Reynolds number of 3×10^6 per foot through the Mach number range from 0.7 to 1.2 in both Tunnels 4T and 16T. The model blockage was 0.606 percent in Tunnel 4T and 0.038 percent in Tunnel 16T. The data of Tunnel 16T are, therefore, considered interference free.

Some data presented herein were taken from a preceding investigation in Tunnel 4T (Ref. 1), and the interference-free data from Tunnel 16T were obtained at the same time as that reported in Ref. 2.

SECTION II
APPARATUS

2.1 TUNNEL 16T

The test facility used to obtain interference-free data is a closed-circuit, continuous flow tunnel with a nominal Mach number range from 0.55 to 1.60. It is capable of operation at stagnation pressures from approximately 100 to 4000 psfa and stagnation temperatures from approximately 90 to 160°F. The removable test section is 16 ft square and 40 ft long. A 9-ft tapered porosity section connects the two-dimensional, solid-plate, flexible nozzle to the perforated-wall test section. The test section walls have 60-deg inclined holes and a porosity of 6 percent which yields near perfect wave cancellation at a Mach number of 1.2. The location of the model in the test section is shown in Fig. 1, Appendix I, and an installation photograph is given as Fig. 2. The model was sting mounted to an auxiliary pitch mechanism which was supported by the main tunnel pitch and roll mechanisms. Additional information on the tunnel may be found in Ref. 3.

2.2 Tunnel 4T

Tunnel 4T is a closed-loop, continuous flow tunnel with a Mach number range from 0.1 to 1.4, a stagnation pressure range from 300 to 3700 psfa, and a stagnation temperature range from 80 to 130°F. The test section flow is generated through a two-dimensional, fixed, sonic-block nozzle with parallel sidewalls. Supersonic speeds are obtained by expansion through the upstream portion of the test section using auxiliary plenum suction. The perforated test section walls are of the variable porosity type with an available porosity range from 0 to 10-percent open area. Two plates with identical hole geometry are utilized, the airside plate being fixed and the backside or cutoff plate sliding upstream for decreasing porosity. A sketch of the model installation in Tunnel 4T is shown in Fig. 3, and Fig. 4 is an installation photograph. Additional information on Tunnel 4T may be found in Ref. 3.

2.3 TEST ARTICLE

The model consisted of a 1/24-scale F-111A fuselage, horizontal tail, inlet spikes, nozzle plugs, vertical tail, dorsal antenna, and fuselage fairings with a special fixed-sweep wing. The wing incorporated leading and trailing edge flaps which were at the zero setting for this investigation. A sketch showing the basic model dimensions is presented in Fig. 5. To fix boundary-layer transition on the model, silicon-carbide abrasive was adhered near the leading edges of the model components as described in Refs. 1 and 2.

2.4 INSTRUMENTATION

An internal six-component strain-gage balance was used to measure forces and moments on the model, and self-balancing transducers referenced to the tunnel plenum pressure were used to measure the pressure at the base of each nozzle plug and inside the fuselage-sting cavity. Electrical signals from the balance, pressure transducers, and standard tunnel instrumentation systems were processed by the PWT data acquisition system and digital computer for on-line data reduction. The balance outputs were also recorded on an oscillograph for monitoring of model dynamics.

SECTION III
TEST DESCRIPTION

3.1 PROCEDURE

Data were obtained in both Tunnels 4T and 16T at nominal test section Mach numbers of 0.7, 0.8, 0.9, 1.0, 1.1, and 1.2. Stagnation temperatures were maintained at approximately 120°F and nominally constant Reynolds numbers of 3 x 10^6 per foot were held by specific stagnation pressure settings. For the results presented here, the model pitch angle ranged from -3 to 10 deg, and roll angles of 0 and 180 deg were used. In Tunnel 16T the model was rolled on line, whereas in Tunnel 4T the 180-deg roll was accomplished by manually breaking the sting/strut connection and reinstalling the model, balance, and sting in the inverted position.

For subsonic Mach numbers in Tunnel 4T, data were obtained at wall porosities of 2, 4, 6, 8, and 10 percent, whereas at supersonic Mach numbers, only 6-percent and optimum settings were used. The optimum wall porosity is the setting which minimizes wave reflections from the walls for a cone-cylinder body of 1-percent blockage (Ref. 4), and this optimum is a function of Mach number; specifically, $\tau = 1.5$ at $M = 1.0$, $\tau = 2.5$ at $M = 1.1$, and $\tau = 4.8$ at $M = 1.2$. In general, a desired Mach number was set and then pitch-polars were made at each of the wall porosity settings.

3.2 DATA REDUCTION

Measured force and moment data were reduced to coefficient form in the stability axes system through the moment reference station shown in Fig. 5 which was at the 0.25 mean aerodynamic chord point. Forebody drag coefficients were obtained by correcting the measured drag for fuselage and nozzle plug base drags and for the internal duct drag. The internal drag corrections were obtained during a previous test in Tunnel 4T (Ref. 1) and applied as a function of Mach number and angle of attack.

The data were corrected for tunnel flow angularities using the mean angle of zero lift as discussed in Section 4.2.

3.3 PRECISION OF MEASUREMENTS

The estimated precision of the data based on the 95-percent confidence level is given in the following table for the two tunnels at M = 0.7 and 1.2. The error sources considered for the coefficients were balance uncertainties, gage zero shifts, Mach number nonuniformities, and Mach number calibration accuracies.

	Tunnel 16T		Tunnel 4T	
	$M_\infty = 0.7$	$M_\infty = 1.2$	$M_\infty = 0.7$	$M_\infty = 1.2$
ΔM_∞	±0.0032	±0.0081	±0.0058	±0.0104
ΔC_D	±0.0043	±0.0045	±0.0029	±0.0031
ΔC_L	±0.0129	±0.0172	±0.0170	±0.0201
ΔC_m	±0.0082	±0.0084	±0.0099	±0.0100
$\Delta\alpha$, deg	±0.1	±0.1	±0.1	±0.1
$\Delta\tau$	---	---	±0.05	±0.05

Limited tunnel calibration data are available at large wall porosities, and the data presented herein for $\tau = 10$ are, therefore, to be examined with caution. In particular, the base drag values for all data at $\tau = 10$ were of opposite sign from the norm which implies a grossly incorrect tunnel pressure ratio for that wall porosity.

SECTION IV
RESULTS AND DISCUSSION

4.1 REFERENCE DATA

Interference-free data obtained in Tunnel 16T are shown in Fig. 6. A model-inverted run was made only at $M_\infty = 0.9$, and these data indicate a Tunnel 16T flow angularity of 0.1-deg upwash. The auxiliary pitch mechanism was rolled with the model so the apparent angularity was not induced by that mechanism. Detailed comparisons of the data obtained in Tunnels 4T and 16T resulted in the conclusions that the effective flow angularity in Tunnel 16T is constant at 0.1-deg upwash for $M_\infty = 0.7$ through 0.9 and that there is no measurable angularity for $M_\infty = 1.0$ through 1.2. This decay to zero angularity for supersonic Mach numbers is not supported by tunnel calibration data, the latter indicating a nearly constant angle throughout the Mach number range.

The curves drawn in Fig. 6 are fairings of the data adjusted for the apparent flow angularity, and these same curves are repeated for comparative purposes on the figures for the Tunnel 4T results.

It is unfortunate, but balance zero shifts occurred during this portion of the Tunnel 16T test which were several times larger than occurred at other times. The end result of these shifts is that the absolute levels of the interference-free data are not as precise as would be desired, although the relative variations of the data within a given pitch polar should not be affected by the balance shifts. In particular, the slopes ($dC_L/d\alpha$ and dC_m/dC_L) of the data are considered to be considerably more precise than the error estimates given in Section 3.3 would indicate. However, the drag data are directly affected by the shifts, and comparisons between Tunnel 4T and 16T data should be made with caution.

Reference 2 presents data obtained at Reynolds numbers of 3.0 and 5.2×10^6 per foot with differential flap settings on this model. These data indicate little sensitivity to Reynolds number variation which implies that differences between Tunnel 4T and 16T results for this model should not be attributable to possible differences in stream turbulence levels.

4.2 FLOW ANGULARITY

A representative set of data obtained in Tunnel 4T is shown in Fig. 7. Comparisons of the upright and inverted runs indicate a test section flow angularity of nominally 0.3-deg downwash, varying slightly with wall porosity.

The previous test of this model in Tunnel 4T (Ref. 1) used nonperforated windows in the top wall for purposes of flow visualization, whereas the bottom wall was fully perforated. The same window arrangement was maintained for the present study. However, the unsymmetrical window installation apparently does not contribute to the flow angularity since a test with symmetrical windows (Ref. 5) indicates generally the same angularity as the present study. It is concluded that a significant flow angularity exists in Tunnel 4T and further study is required to isolate and correct the problem.

To simplify analysis of the present results, C_L, C_D, and α were corrected for the apparent tunnel flow angularity. The correction was defined as the difference between the measured angle of zero lift for

each pitch polar and the mean α_0 for each Mach number. The range of the corrections is shown in Fig. 8 with the results of Ref. 5 also shown for comparison.

4.3 EFFECT OF VARIABLE WALL POROSITY

The influence of wall porosity on the stability data in Tunnel 4T is presented in Figs. 9 through 14. The curves in each figure are fairings of the data obtained in Tunnel 16T.

In general, it is possible to obtain nearly interference-free data in Tunnel 4T by selection of a wall porosity schedule as a function of Mach number. Referring to Fig. 9, for example, the correct lift is obtainable with $\tau = 4$ at $M_\infty = 0.7$; however, the drag and pitching moment show slight deviations from the Tunnel 16T data.

The most dramatic demonstration of the effectiveness of variable wall porosity is provided by the results at $M_\infty = 1.0$ (Fig. 12). A wall porosity of 1.5 yields data that are in good agreement with the Tunnel 16T results, whereas the $\tau = 6.0$ data show considerable wall interference effects.

An incidental effect of wall porosity was noted during conduct of the test. For the larger wall porosities and especially at $\tau = 10$, the dynamic oscillations in yaw of the model were noticeably higher in magnitude than noted at $\tau = 6.0$ and below. These oscillations were higher still during transition from one porosity setting to another wherein the walls probably were not at the same uniform porosity.

4.4 EFFECT OF TUNNEL PRESSURE RATIO

The tunnel pressure ratio, λ, for Tunnel 4T is manually controlled, and occasional setting errors occur. To document the effect of tunnel pressure ratio, data were obtained at $M_\infty = 0.7$ with λ settings corresponding to those for $M_\infty = 0.6$ and 0.8. The results are presented in Fig. 15, and no significant discrepancies are evident. However, the model base pressures were slightly influenced by the different λ settings which resulted in a consistent base drag variation from 40 percent below to 30 percent above the nominal Tunnel 16T value.

4.5 BLOCKAGE EFFECTS

Data are presented in Ref. 4 which demonstrate significant subsonic blockage interference with a 1-percent blockage model at low wall porosities. Unpublished data have since been obtained with a 1.6-percent blockage model which indicated roughly twice the amount of blockage interference. Judicious extrapolation from these two data points to the present 0.6-percent blockage model results in the conclusion that the maximum subsonic blockage interference effect on the present data is on the order of 1 percent. This effect is thus buried in the data inaccuracies and could not be isolated.

With regard to transonic blockage, Ref. 4 indicates that $\tau = 1.5$ is optimum for a 1-percent blockage model at $M_\infty = 1.0$. The present data at $M_\infty = 1.0$ (Fig. 12) indicate that a smaller wall porosity setting might be beneficial which implies that the optimum wall porosity at $M_\infty = 1.0$ is a slight function of model blockage.

4.6 SUBSONIC LIFT INTERFERENCE EFFECTS

The effects of wall porosity on the slopes of the lift and pitching-moment data are shown in Figs. 16 and 17. These results were obtained by fitting a least-squares line to the data shown in Figs. 9, 10, and 11 for angles of attack less than $\alpha = 1$ and then subtracting the corresponding Tunnel 16T result. The theoretical curves in the figures are the expected interference effects for the model in Tunnel 4T as developed in Appendix II.

In general, the data and theory are in qualitative agreement; and at $M_\infty = 0.7$ (Fig. 16), data and theory agree quantitatively as well. However, with increasing Mach number a discrepancy is evident which implies that the theoretical compressibility correction is not adequate. As discussed in Appendix II, the theoretical curves for the pitching moment slope are not as well founded as those for lift; and the indicated disagreement between theory and experiment may be exaggerated.

The fairings of the data in Figs. 16 and 17 were made without considering the results at the higher wall porosities.

4.7 RECOMMENDED WALL POROSITY SCHEDULE

Intersection of the faired experimental data in Figs. 16 and 17 with the zero line yields a wall porosity at each Mach number which provides

an interference-free test condition. These points are presented in Fig. 18 and compared with the theoretically required porosities as developed in Appendix II.

The porosity schedule required to eliminate induced upwash interference is labeled $\delta_0 = 0$, and the schedule which theoretically eliminates streamline curvature interference is designated by $\delta_1 = 0$. The schedules are not the same so that, in general, there is no way to completely eliminate interference effects in Tunnel 4T. However, for aircraft models, the induced upwash is the predominant lift interference effect which allows practical achievement of interference-free data by utilizing the porosity schedule for $\delta_0 = 0$.

The recommended Tunnel 4T wall porosity schedule for subsonic Mach numbers is, therefore, the theoretical schedule for $\delta_0 = 0$ with adjustment in the transonic range which matches the requirements determined by Ref. 4 and the present results.

The recommended schedule of Ref. 4 for supersonic operation is modified slightly because of the excellent agreement of theory and experiment at the Mach numbers where sufficient data were obtained.

SECTION V
CONCLUSIONS

The investigation to document the quality of data obtained in the PWT Aerodynamic Wind Tunnel (4T) utilizing a 0.6-percent blockage fighter-type model has resulted in the following conclusions:

1. Practically interference-free static stability data are obtainable throughout the Mach number range from M = 0.7 to 1.2 using the recommended variable wall porosity schedule.
2. A nominally constant flow angularity of 0.3-deg downwash exists for M = 0.7 through 1.2.
3. Small variations in tunnel pressure ratio have no discernible effect on static stability data.
4. At other than the optimum wall porosities, experimental subsonic lift interference effects are generally larger than theoretical predictions, although theory and experiment are in qualitative agreement.

REFERENCES

1. Butler, Richard W. and Lehner, Paul. "Aerodynamic Characteristics of Wing-Mounted Devices for Producing Roll Control with High Lift at Transonic Speeds." AEDC-TR-69-273 (AD863418), December 1969.

2. Price, Earl A., Jr. "Aerodynamic Characteristics of a Fixed-Wing Fighter-Type Aircraft Employing Various Roll-Control Devices at Transonic Mach Numbers." AEDC-TR-69-258 (AD862675), December 1969.

3. Test Facilities Handbook (Eighth Edition). "Propulsion Wind Tunnel Facility, Vol. 5." Arnold Engineering Development Center, December 1969.

4. Jacocks, J. L. "Determination of Optimum Operating Parameters for the AEDC-PWT 4-ft Transonic Tunnel with Variable Porosity Test Section Walls." AEDC-TR-69-164 (AD857045), August 1969.

5. Anderson, C. F. "An Investigation of the Aerodynamic Characteristics of the AGARD Model B for Mach Numbers from 0.2 to 1.0." AEDC-TR-70-100, May 1970.

6. Oliver, Robert H. "Determination of Blockage and Lift Interference for Rectangular Wind Tunnels with Perforated Walls." Master of Science Thesis, University of Tennessee Space Institute, August 1969.

7. Pindzola, M. and Lo, C. F. "Boundary Interference at Subsonic Speeds in Wind Tunnels with Ventilated Walls." AEDC-TR-69-47 (AD687440), May 1969.

8. Rohde, John E., Richards, Hadley T., and Metger, George W. "Discharge Coefficients for Thick Plate Orifices with Approach Flow Perpendicular and Inclined to the Orifice Axis." NASA TN D-5467, October 1969.

9. Ellison, D. E. "USAF Stability and Control DATCOM." (AF Project Engineer, D. E. Hoak), Flight Control Division, Air Force Flight Dynamics Laboratory, Wright-Patterson Air Force Base, Ohio. Revised August 1968.

APPENDIXES

I. ILLUSTRATIONS

II. THEORETICAL LIFT INTERFERENCE EFFECTS

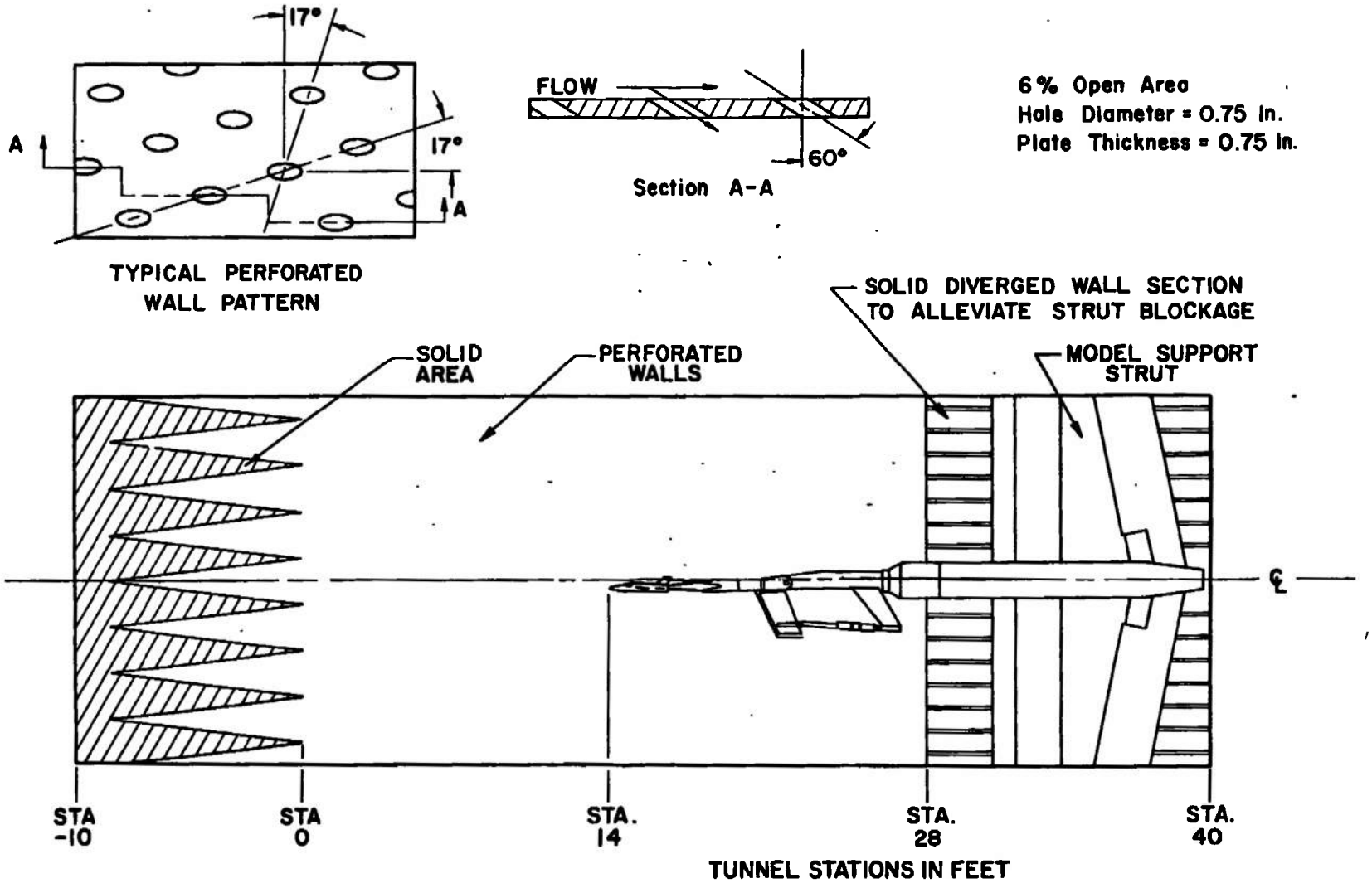

Fig. 1 Model Installation in Tunnel 16T

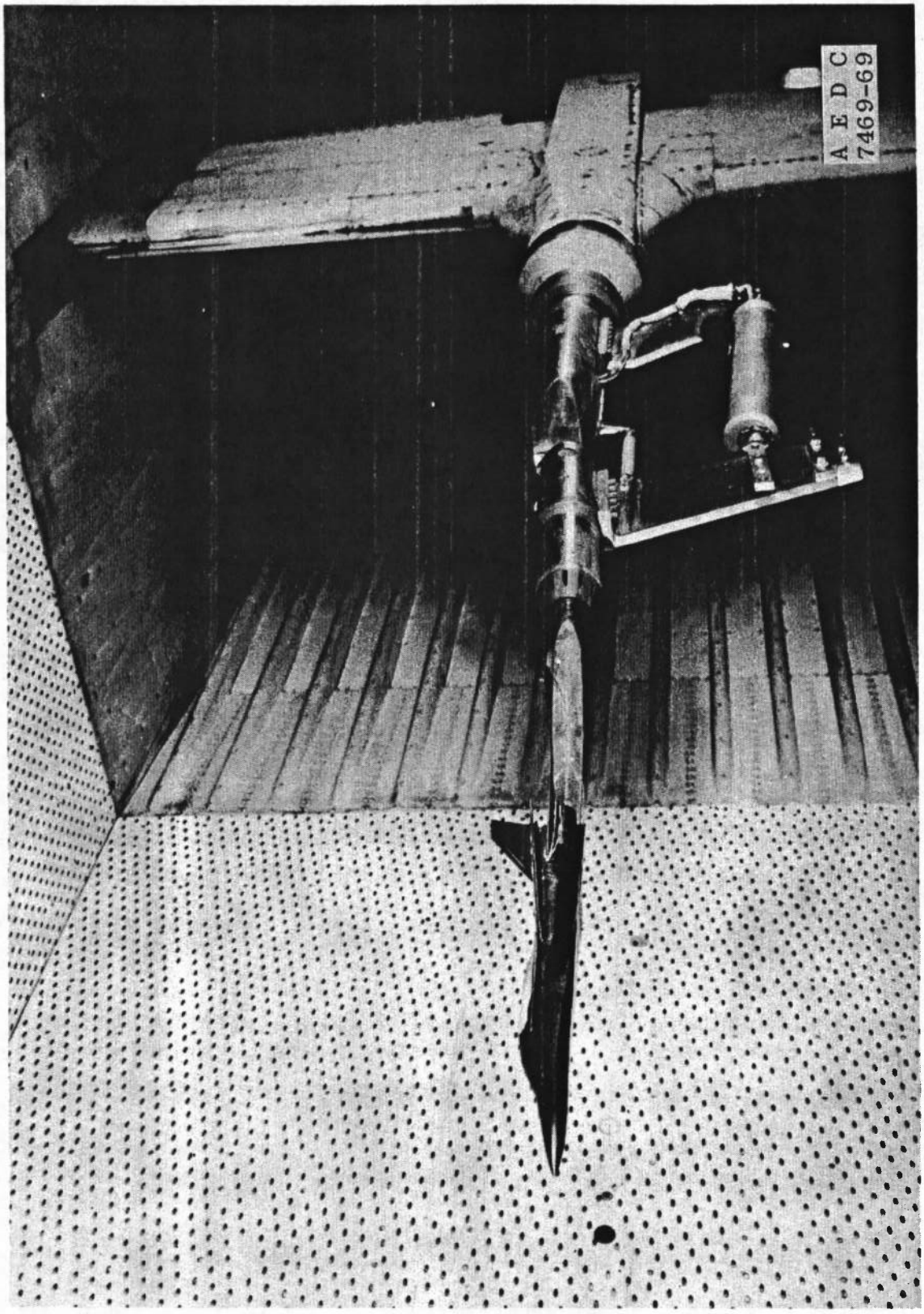

Fig. 2 Photograph of Tunnel 16T Installation

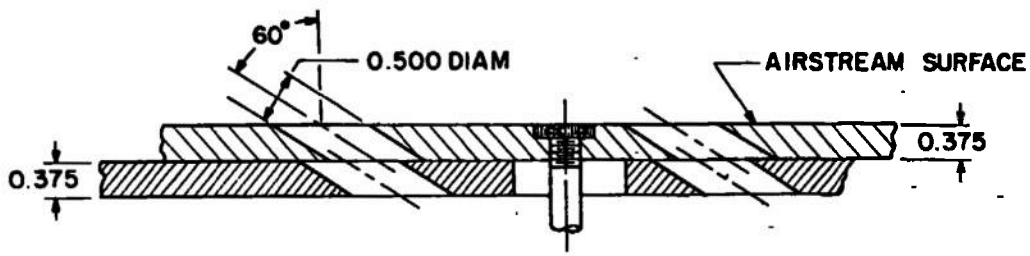

TYPICAL PERFORATED WALL CROSS SECTION

ALL DIMENSIONS IN INCHES

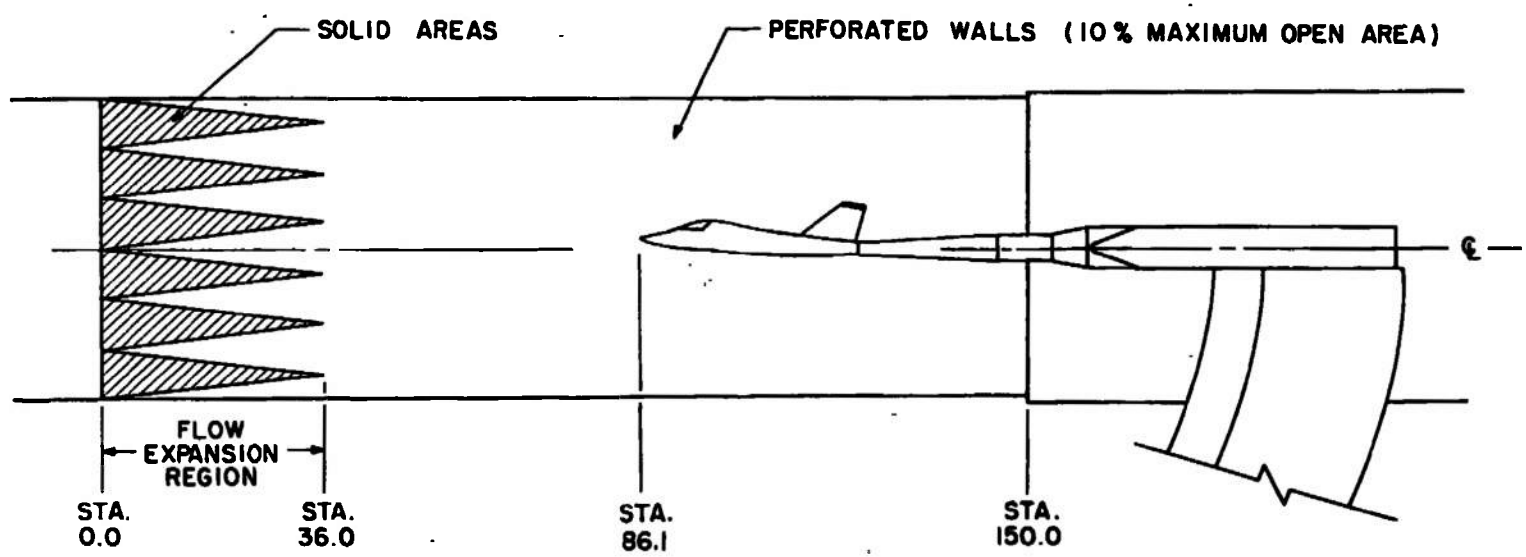

Fig. 3 Model Installation in Tunnel 4T

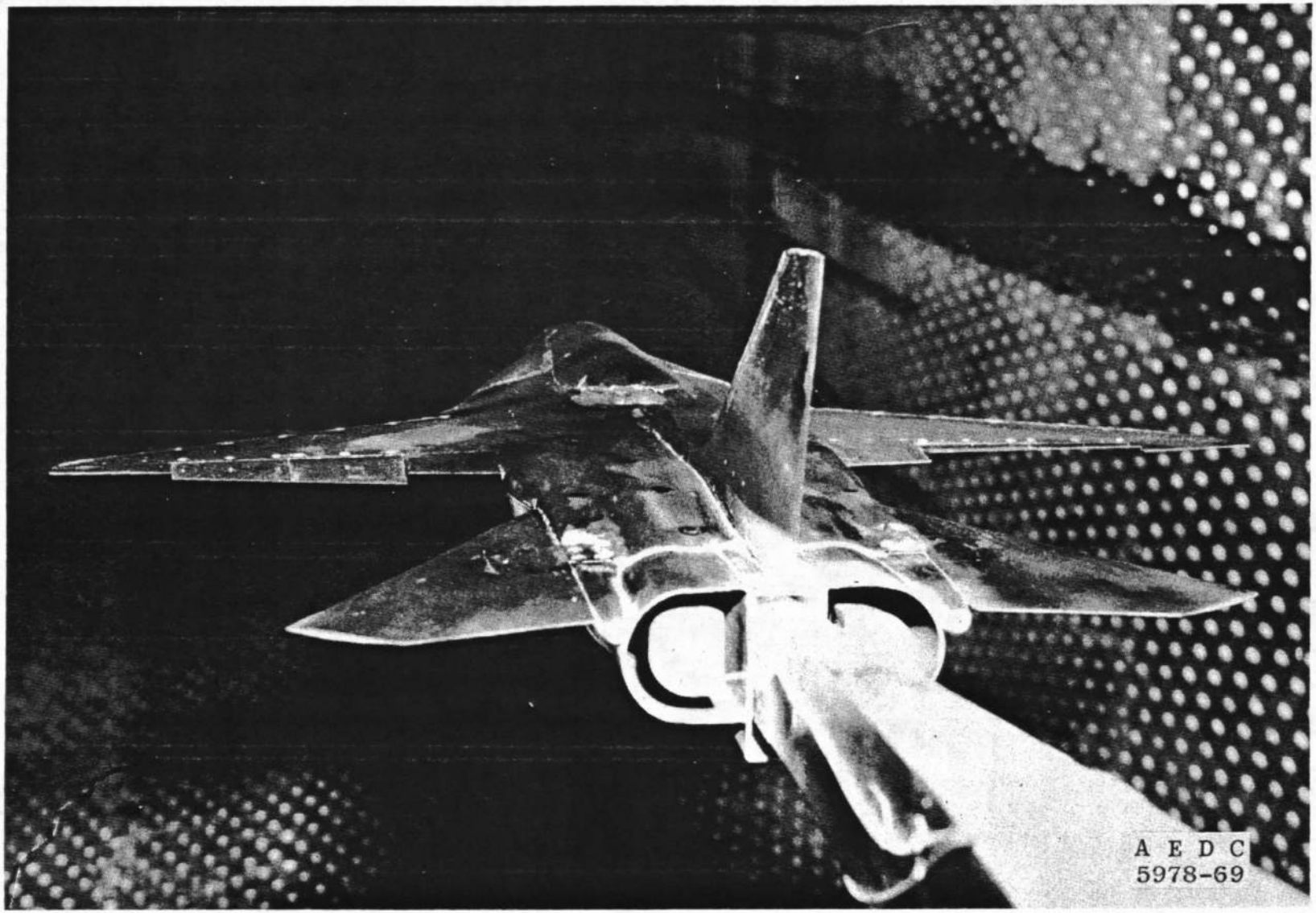

Fig. 4 Photograph of Tunnel 4T Installation

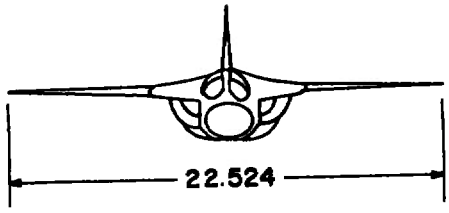

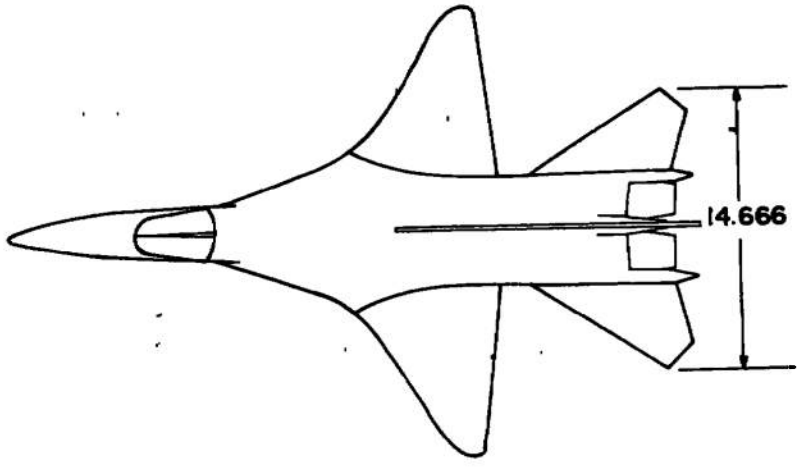

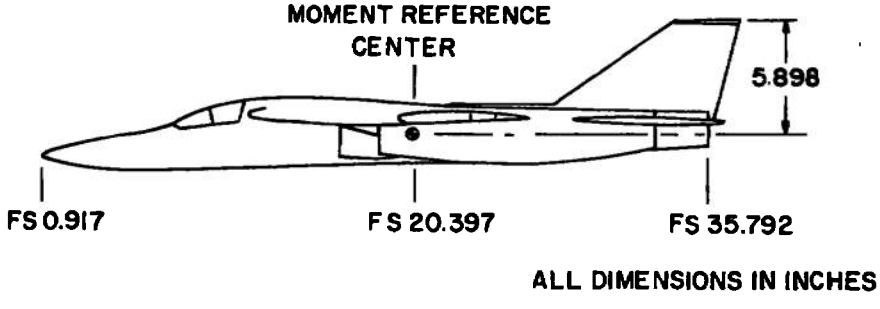

Fig. 5 Dimensional Sketch of the Model

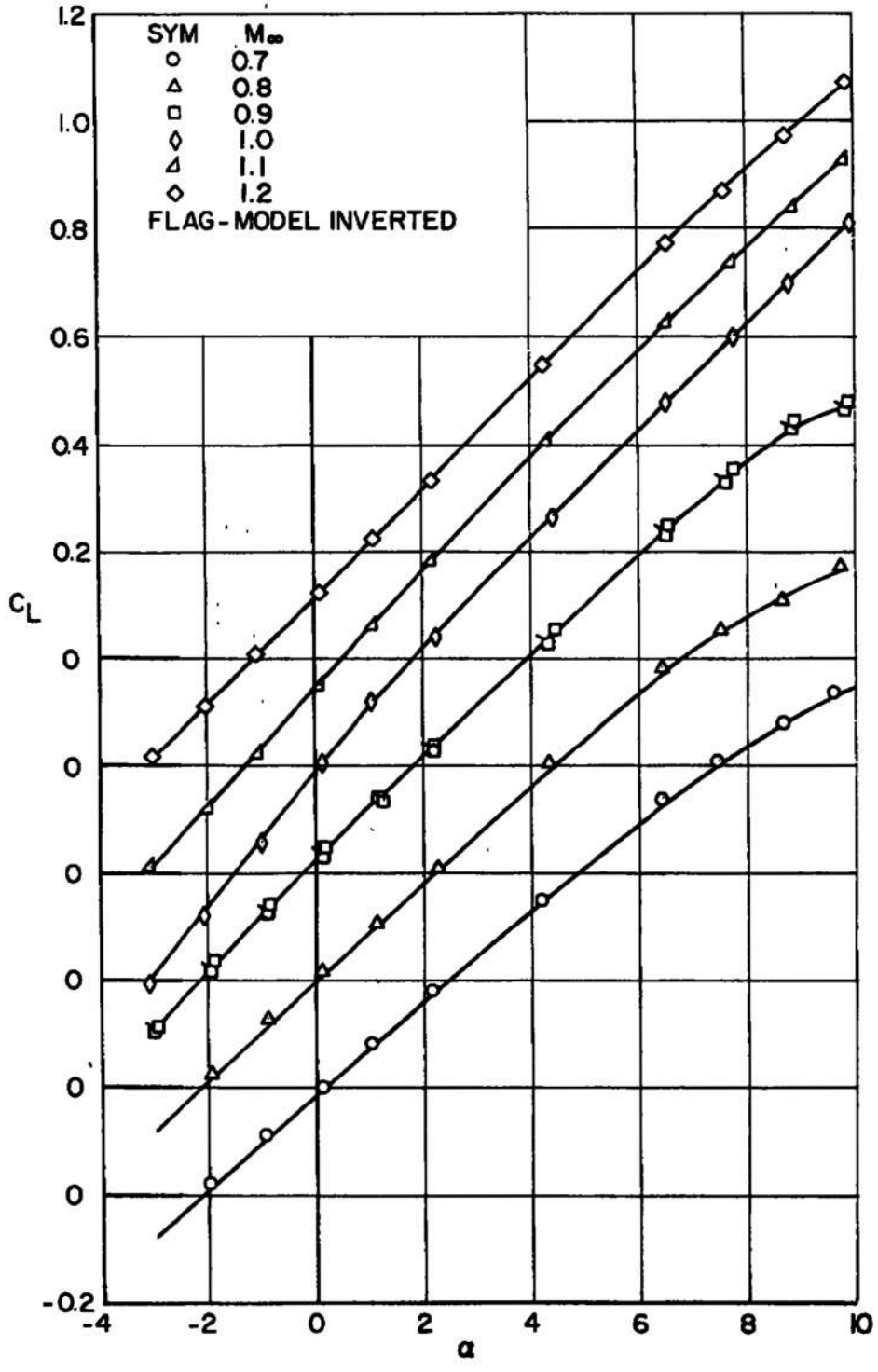

a. Lift

Fig. 6 Interference-Free Results from Tunnel 16T

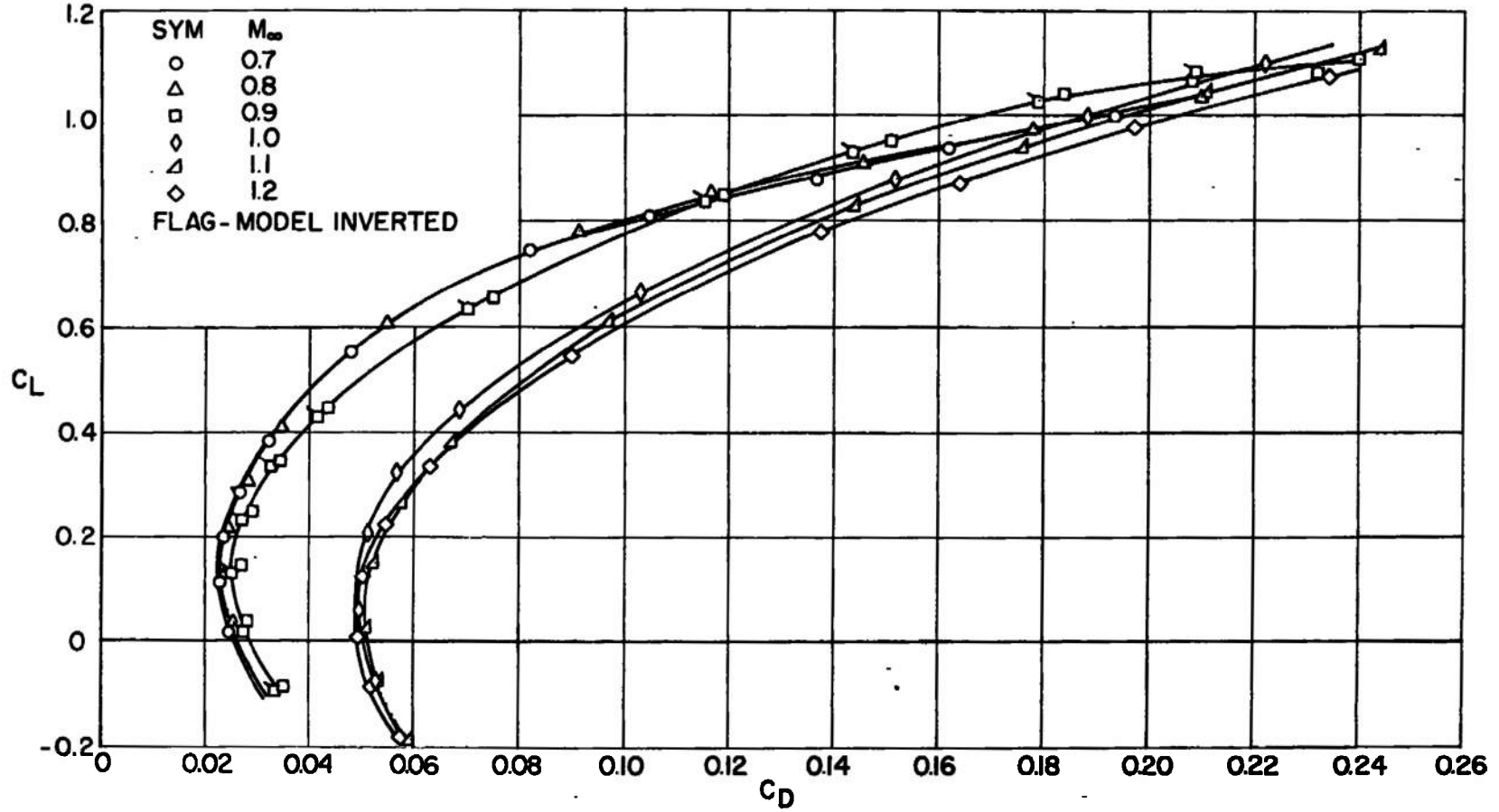

b. Drag

Fig. 6 Continued

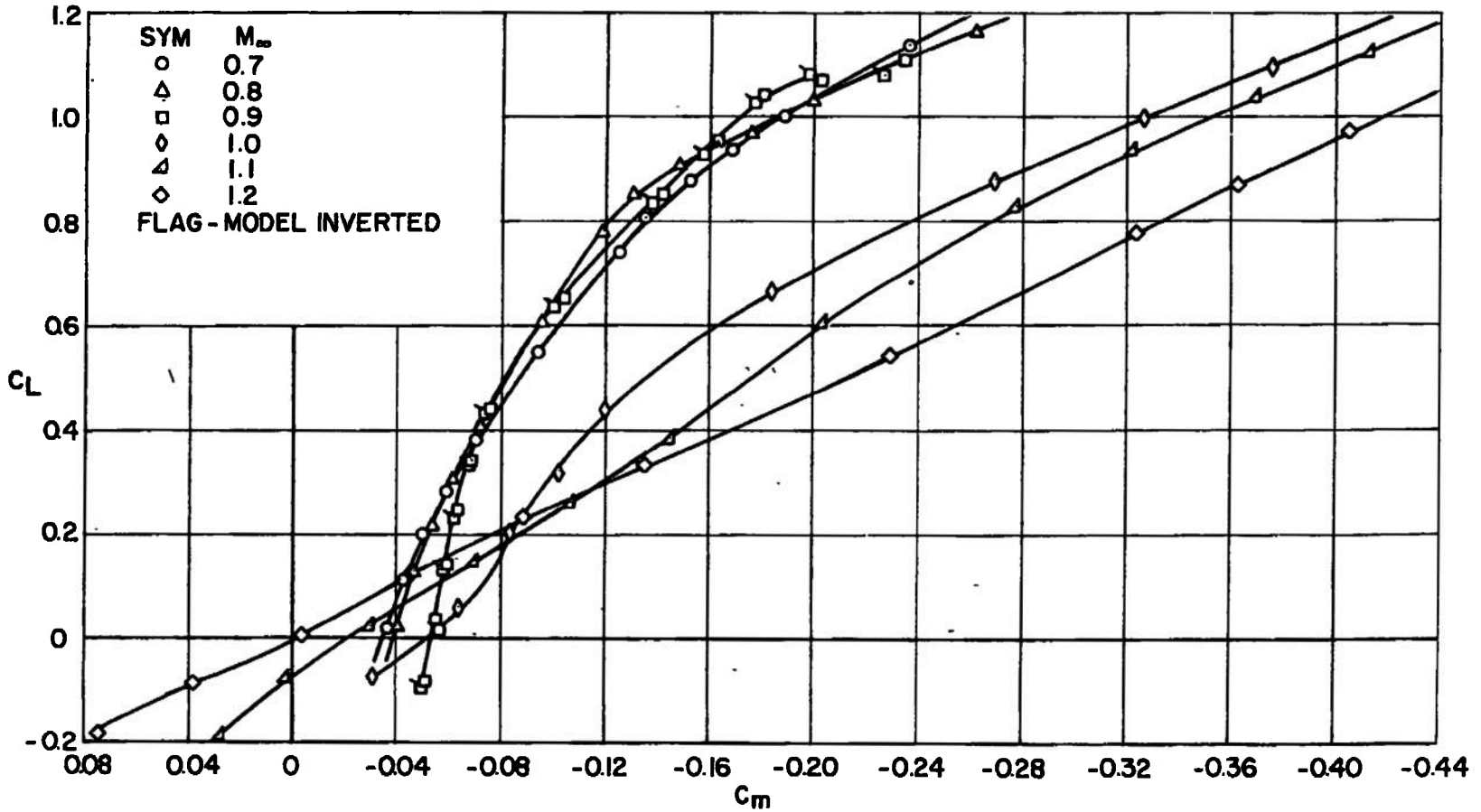

c. Pitching Moment
Fig. 6 Concluded

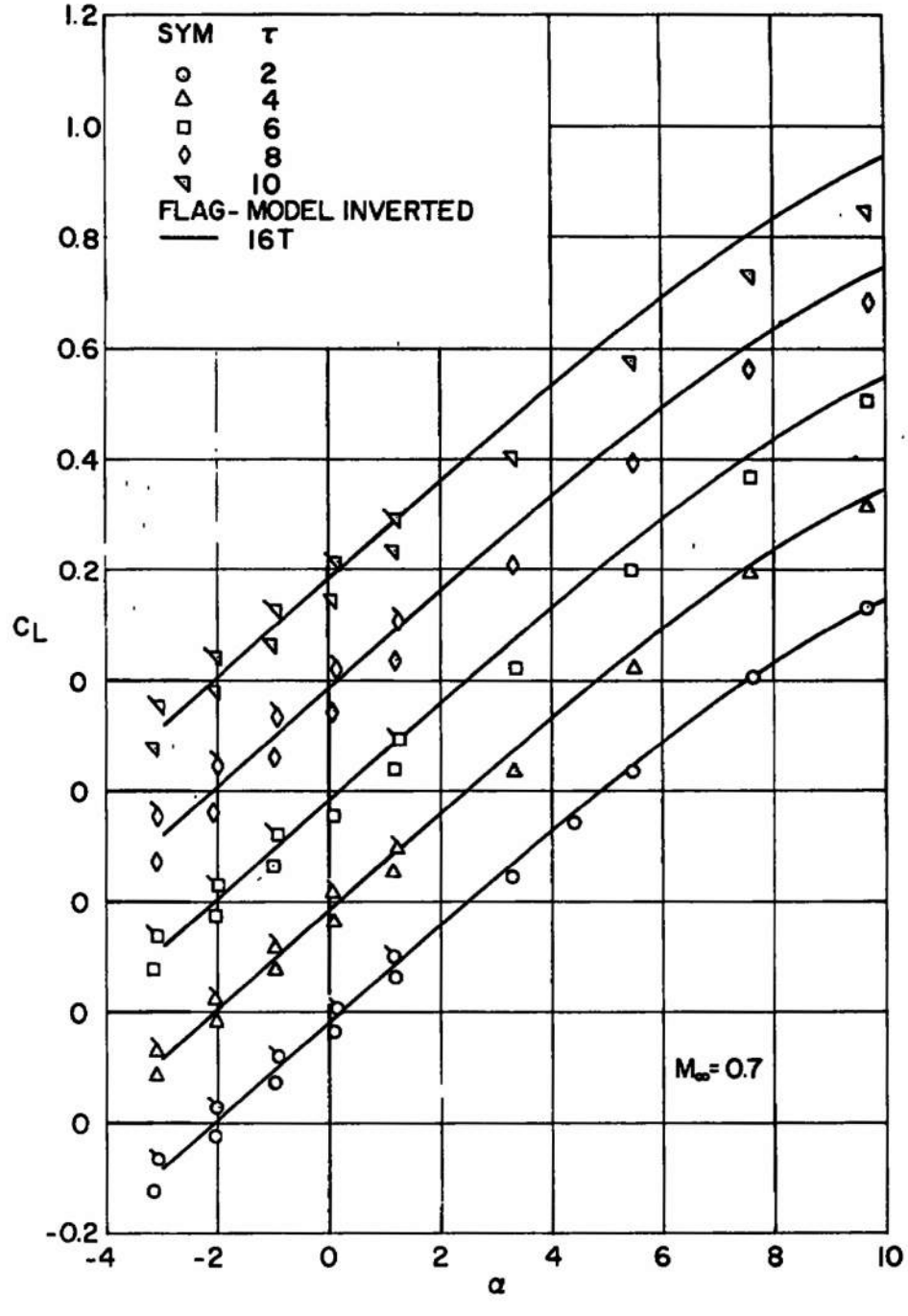

a. Lift

Fig. 7 Uncorrected Data from Tunnel 4T at M_∞ = 0.7

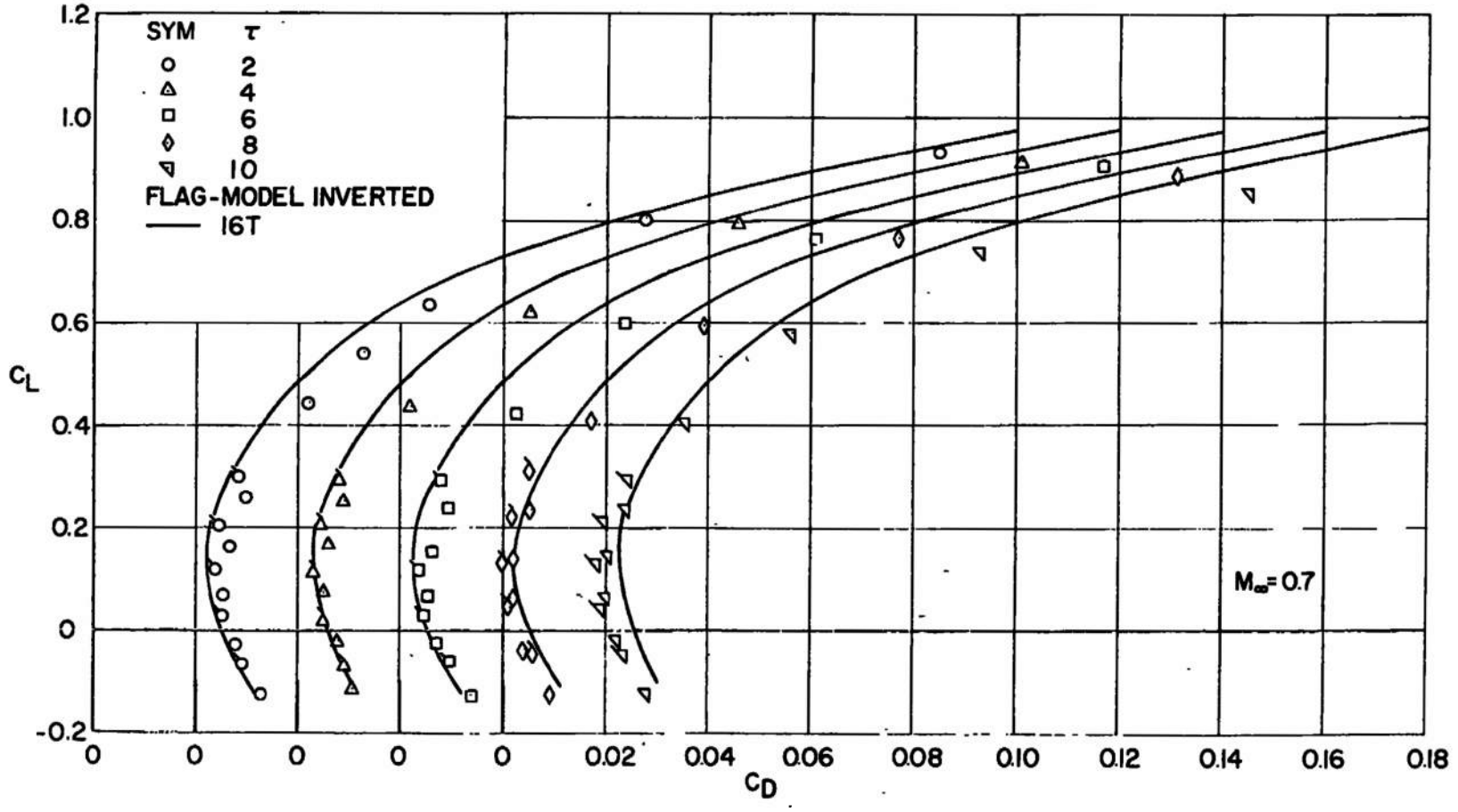

b. Drag
Fig. 7 Continued

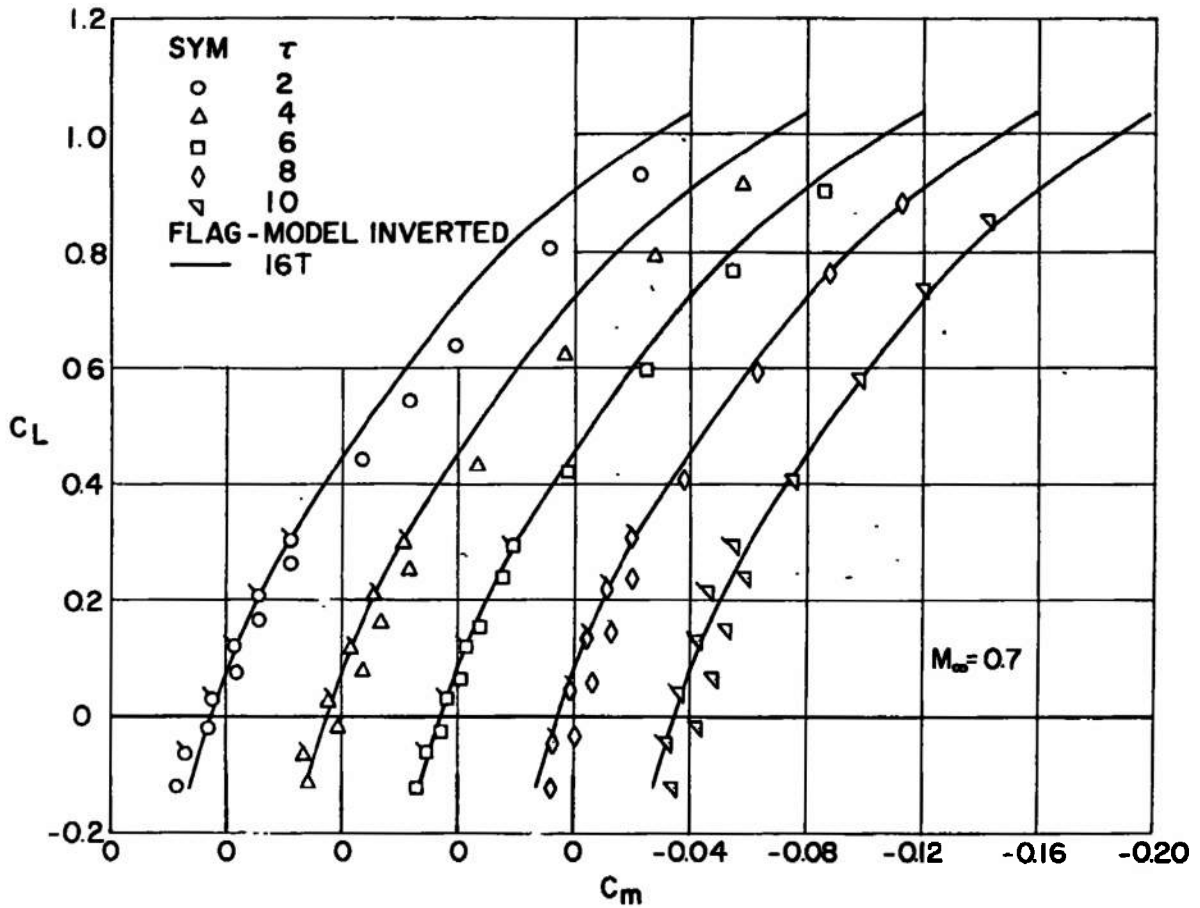

c. Pitching Moment
Fig. 7 Concluded

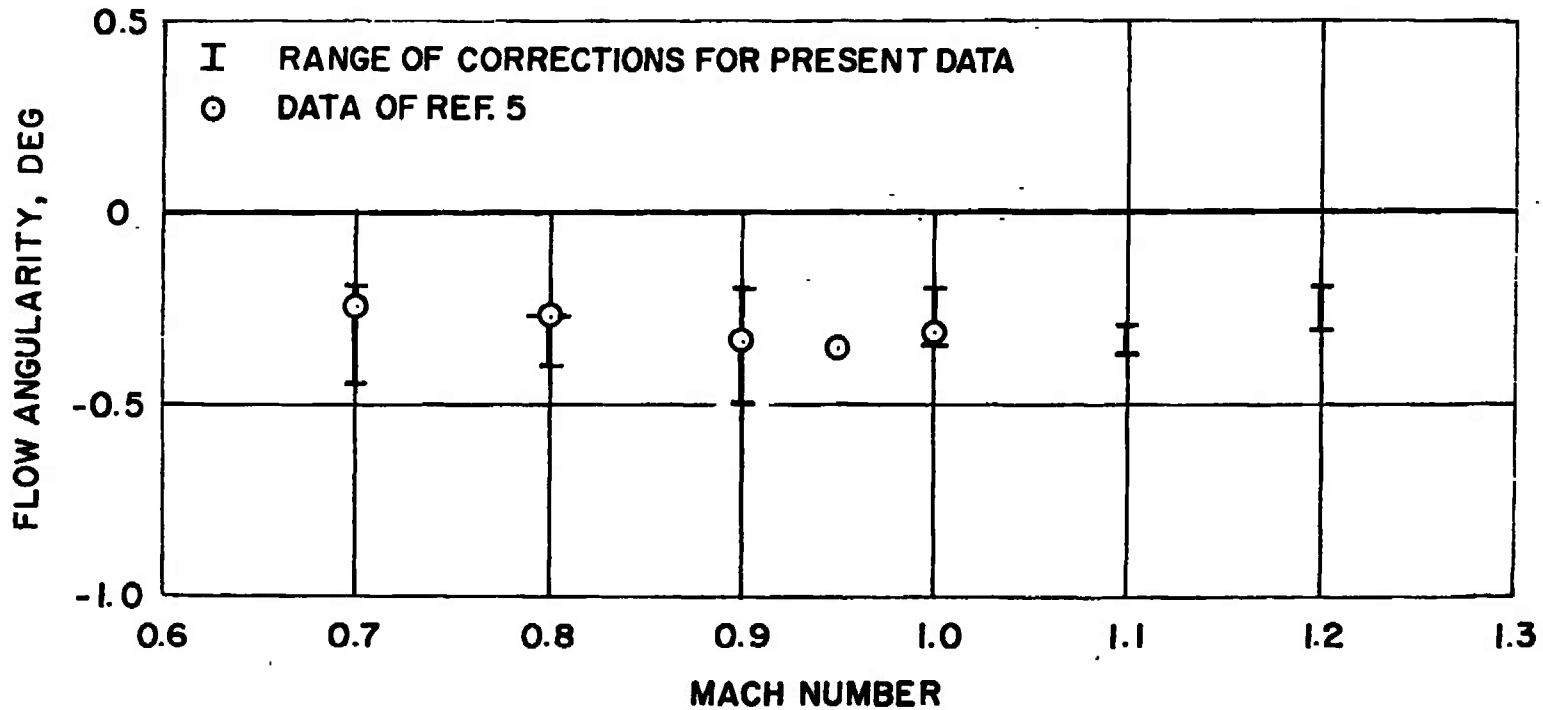

Fig. 8 Tunnel 4T Flow Angularity

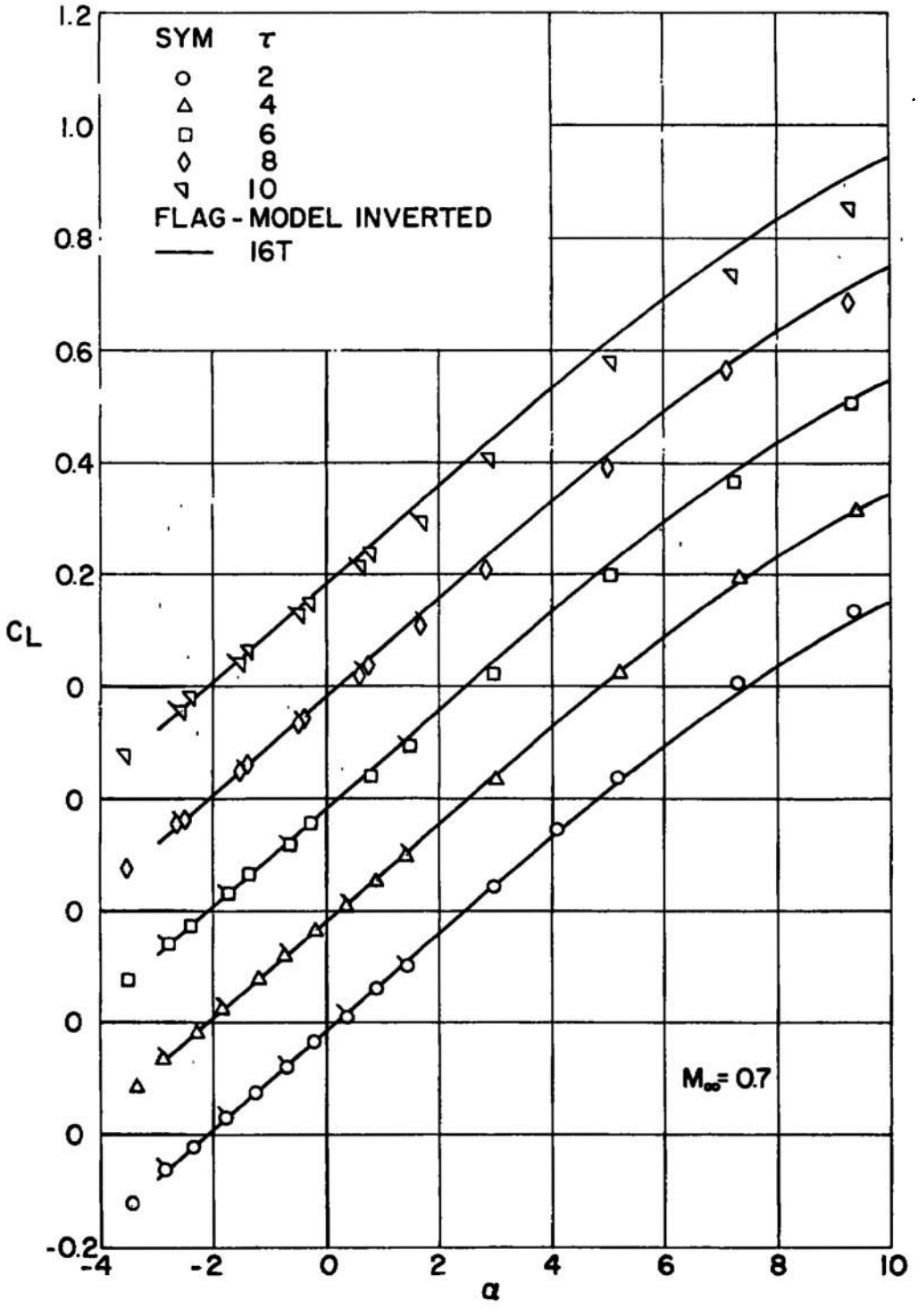

a. Lift

Fig. 9 Effect of Variable Wall Porosity in Tunnel 4T at M_∞ = 0.7

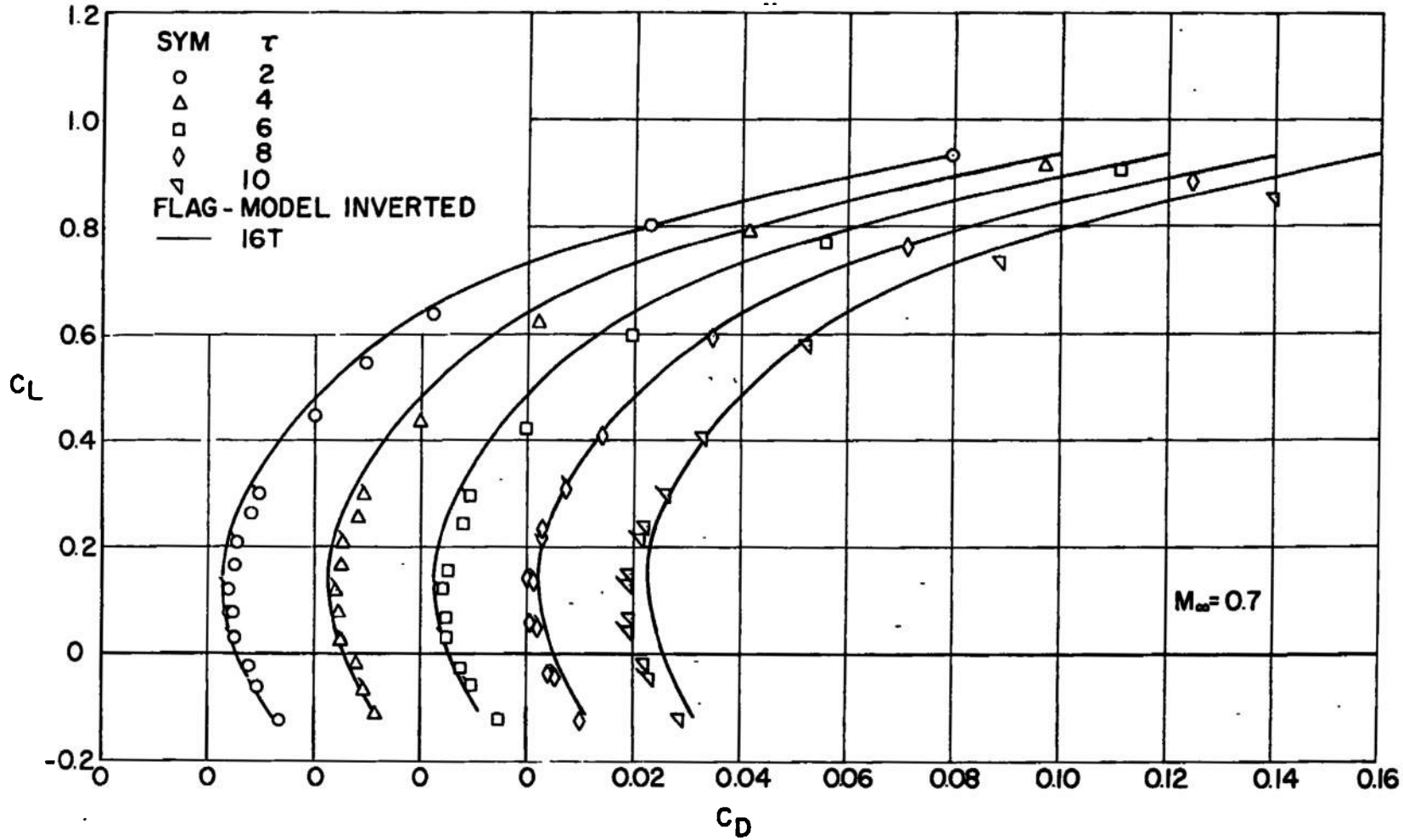

b. Drag

Fig. 9 Continued

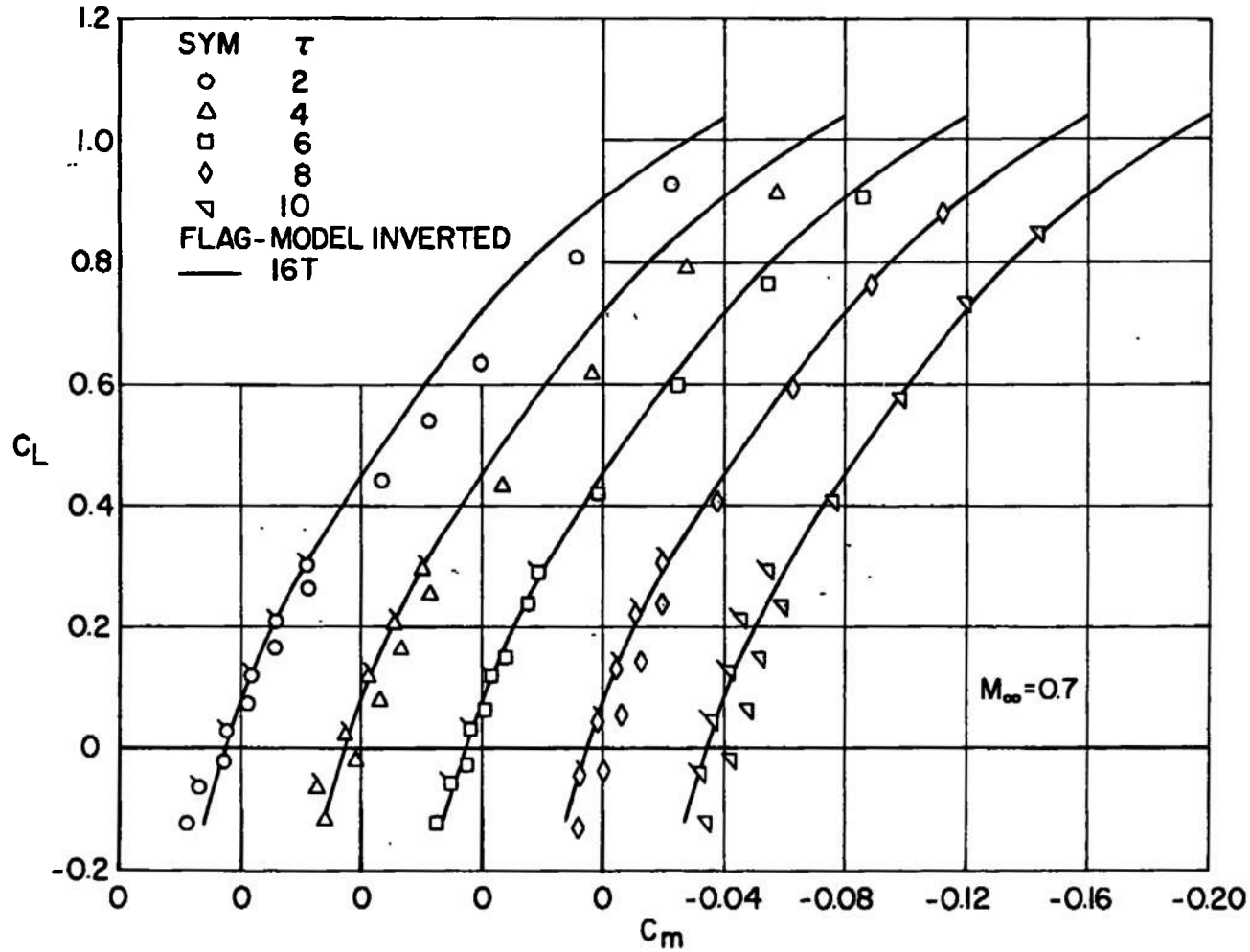

c. Pitching Moment
Fig. 9 Concluded

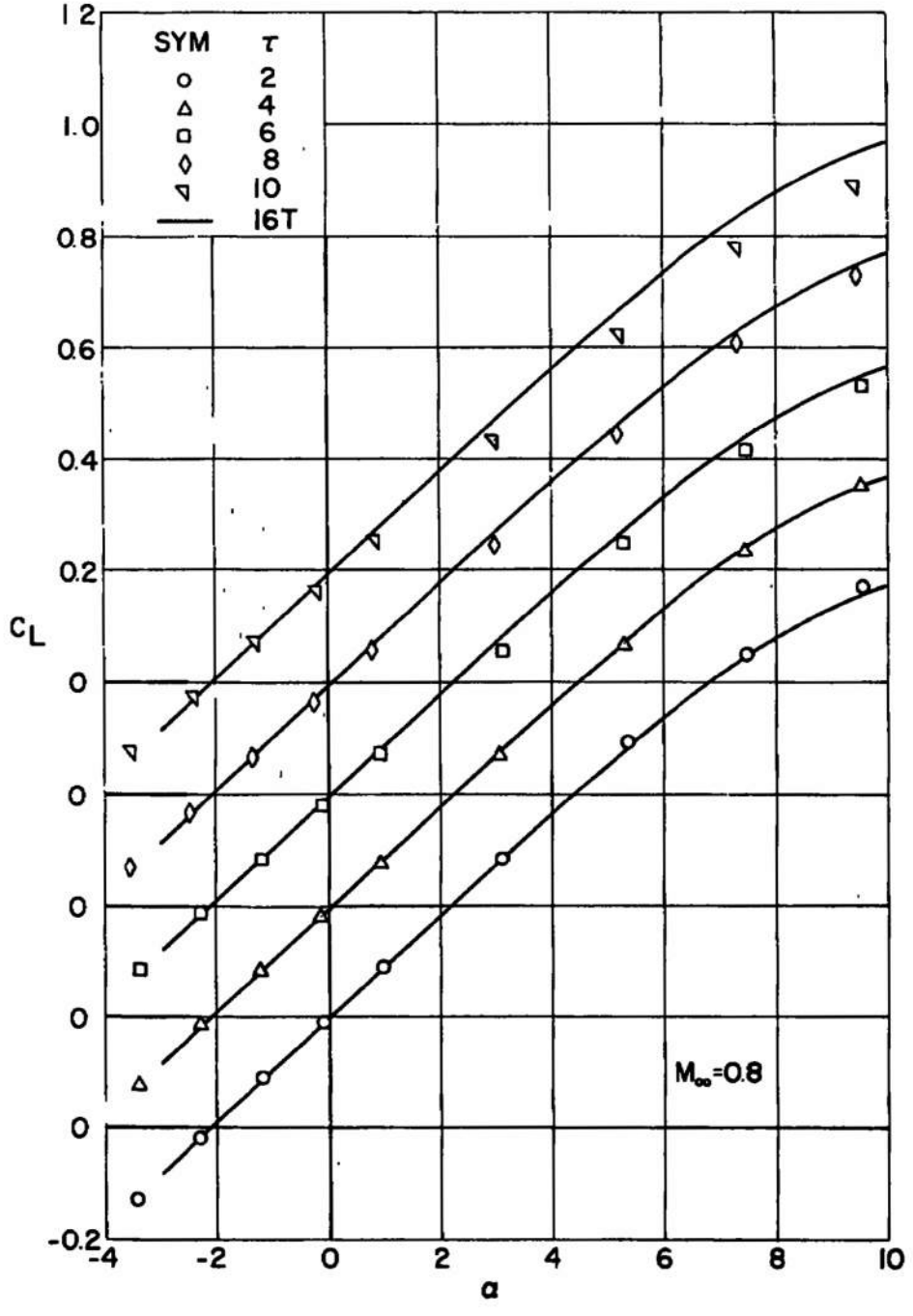

a. Lift

Fig. 10 Effect of Variable Wall Porosity in Tunnel 4T at M_∞ = 0.8

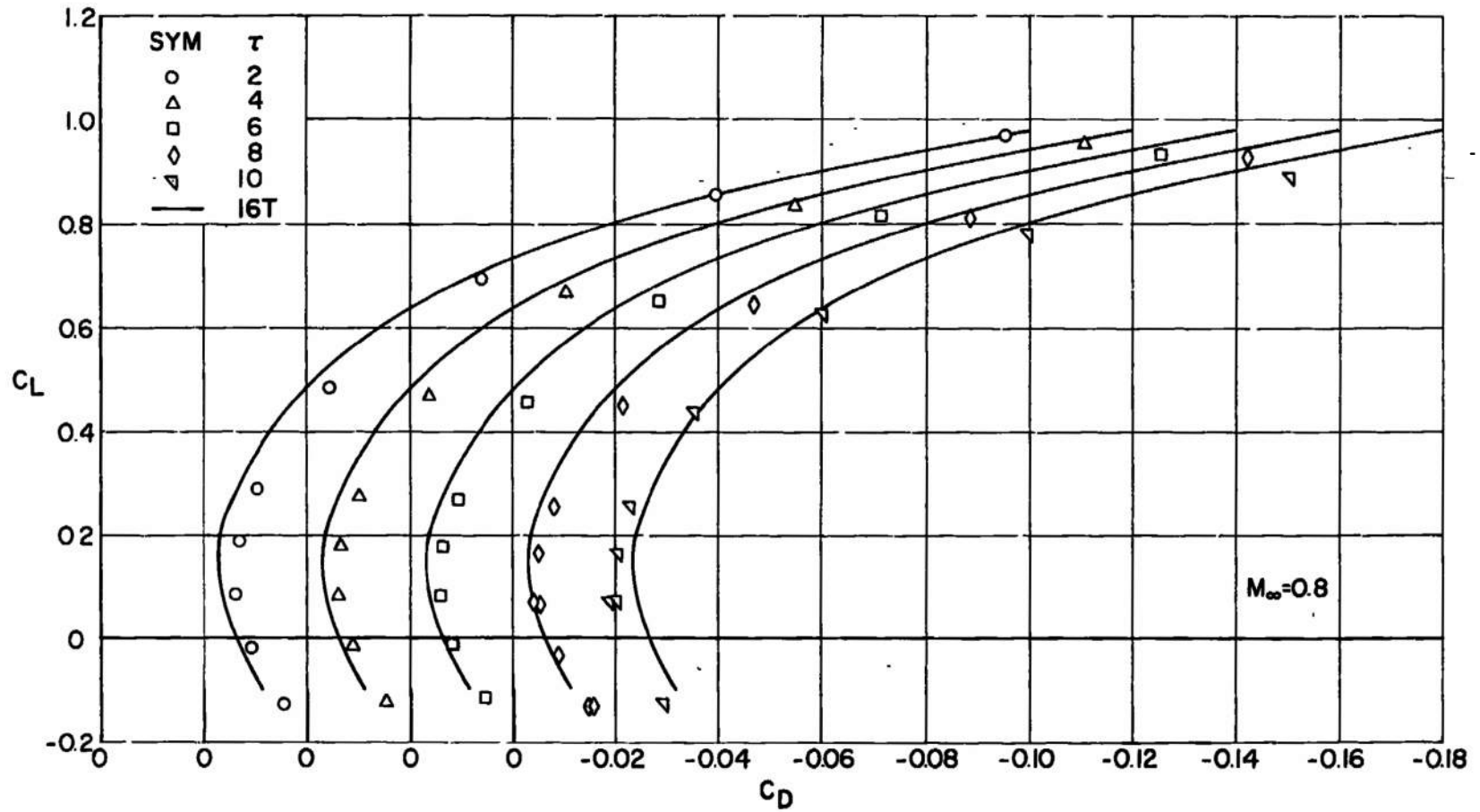

b. Drag

Fig. 10 Continued

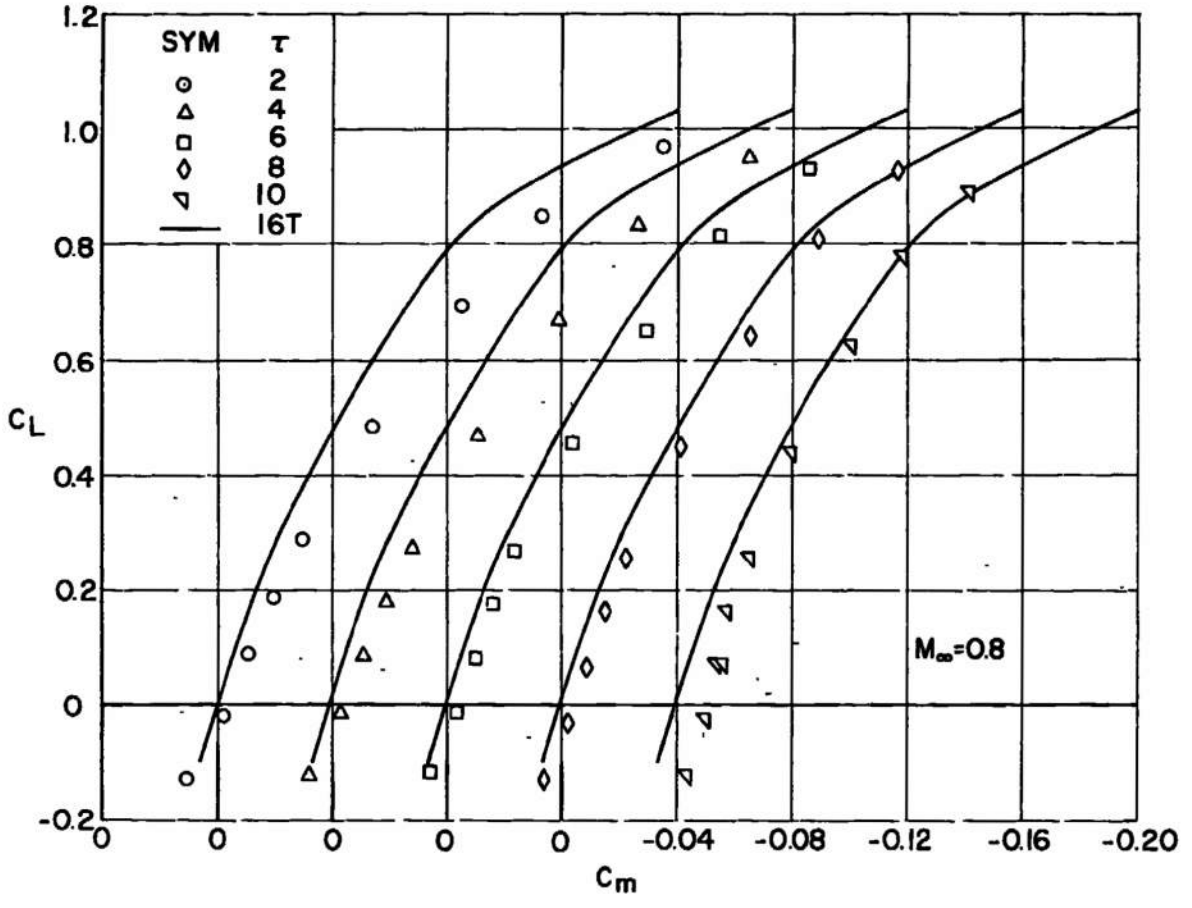

c. Pitching Moment
Fig. 10 Concluded

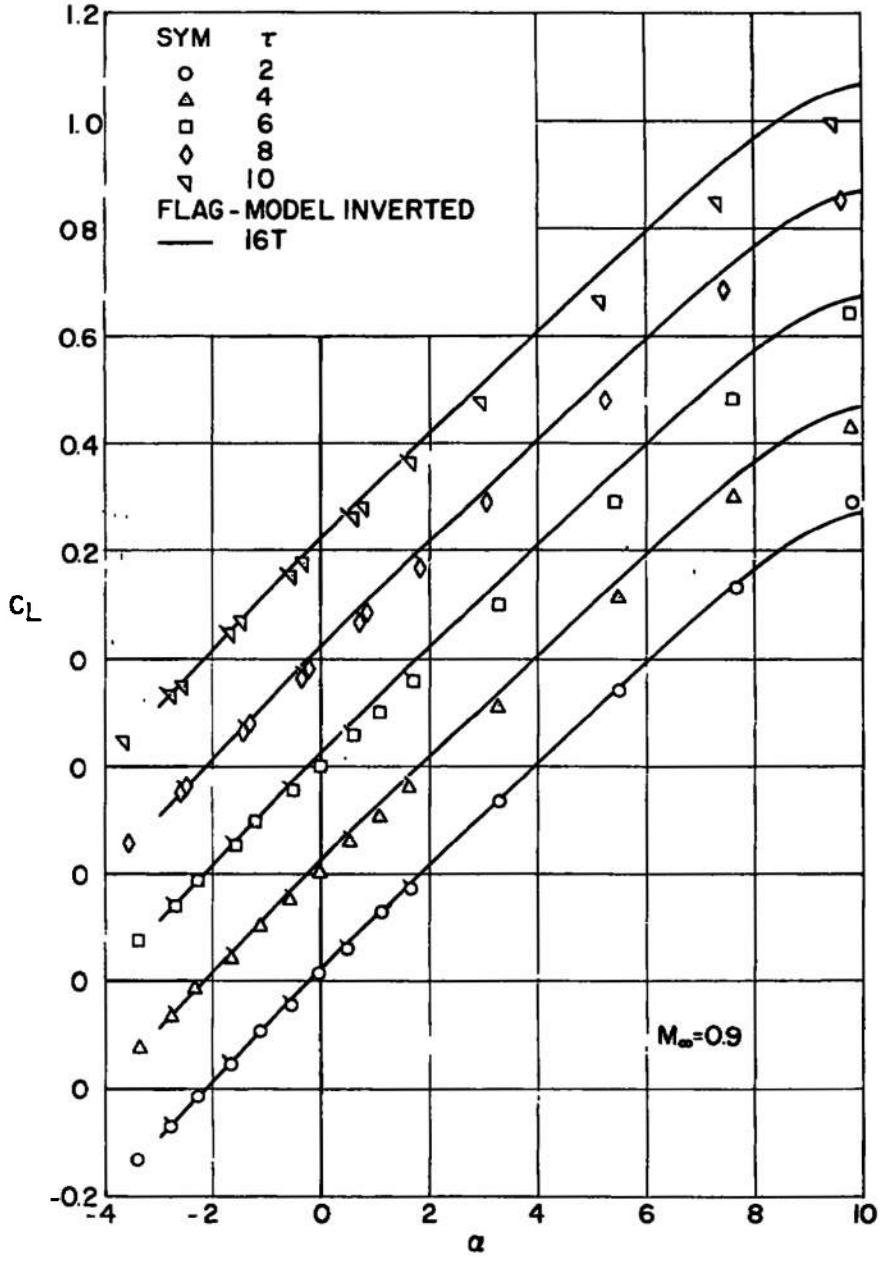

a. Lift

Fig. 11 Effect of Variable Wall Porosity in Tunnel 4T at M_∞ = 0.9

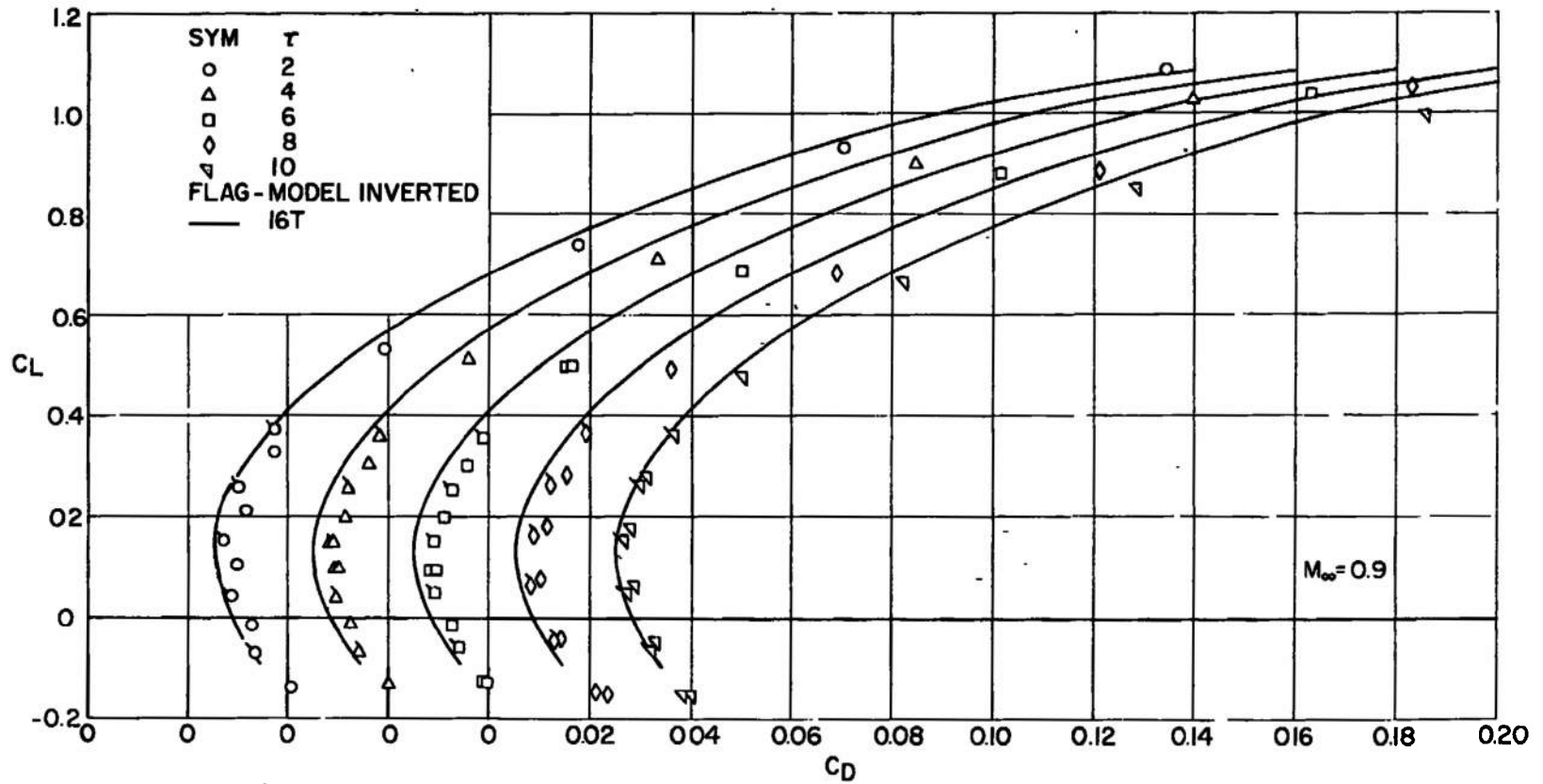

b. Drag

Fig. 11 Continued

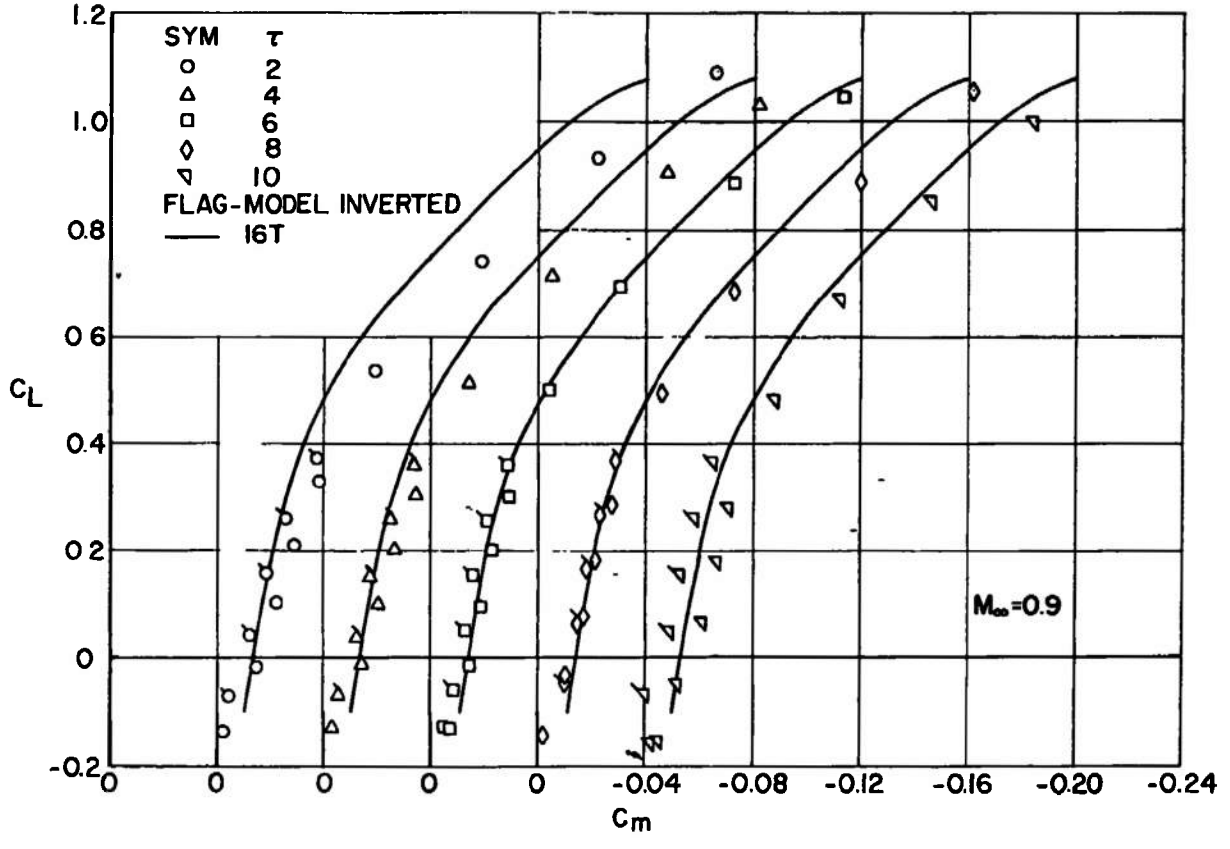

c. Pitching Moment
Fig. 11 Concluded

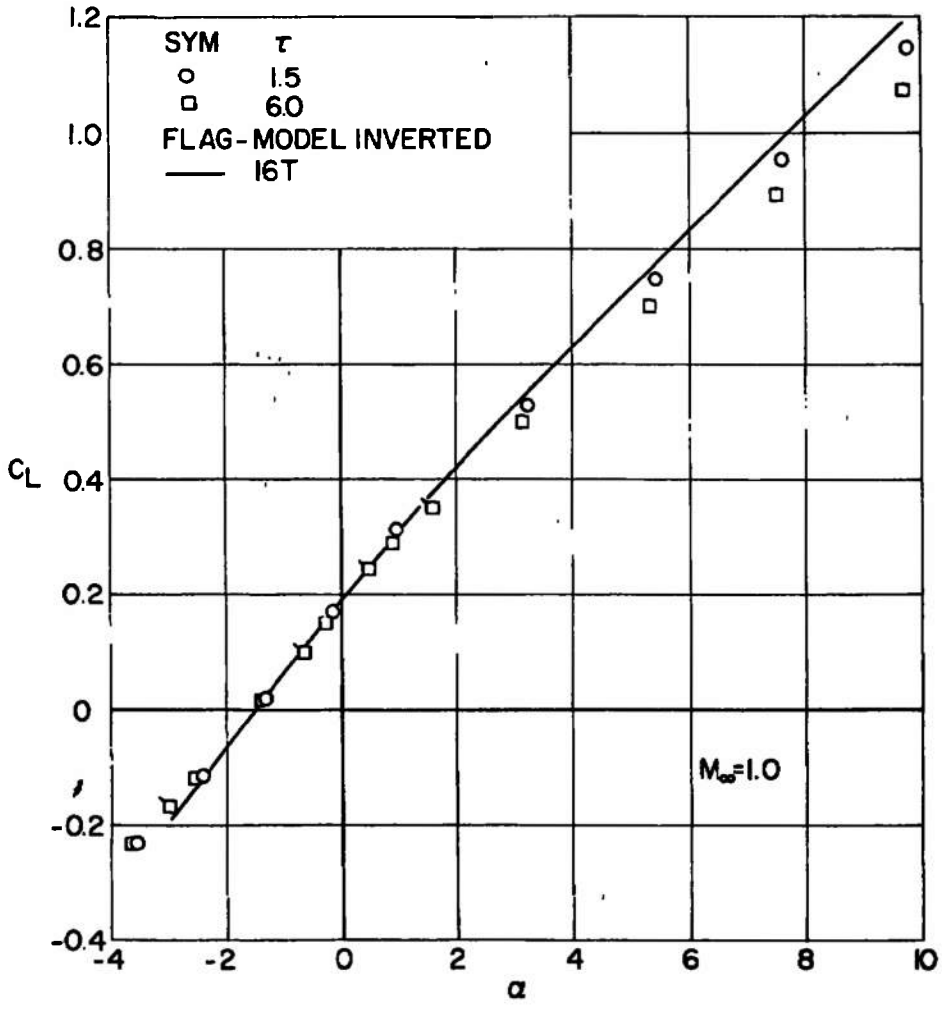

a. Lift

Fig. 12 Effect of Variable Wall Porosity in Tunnel 4T at M_∞ = 1.0

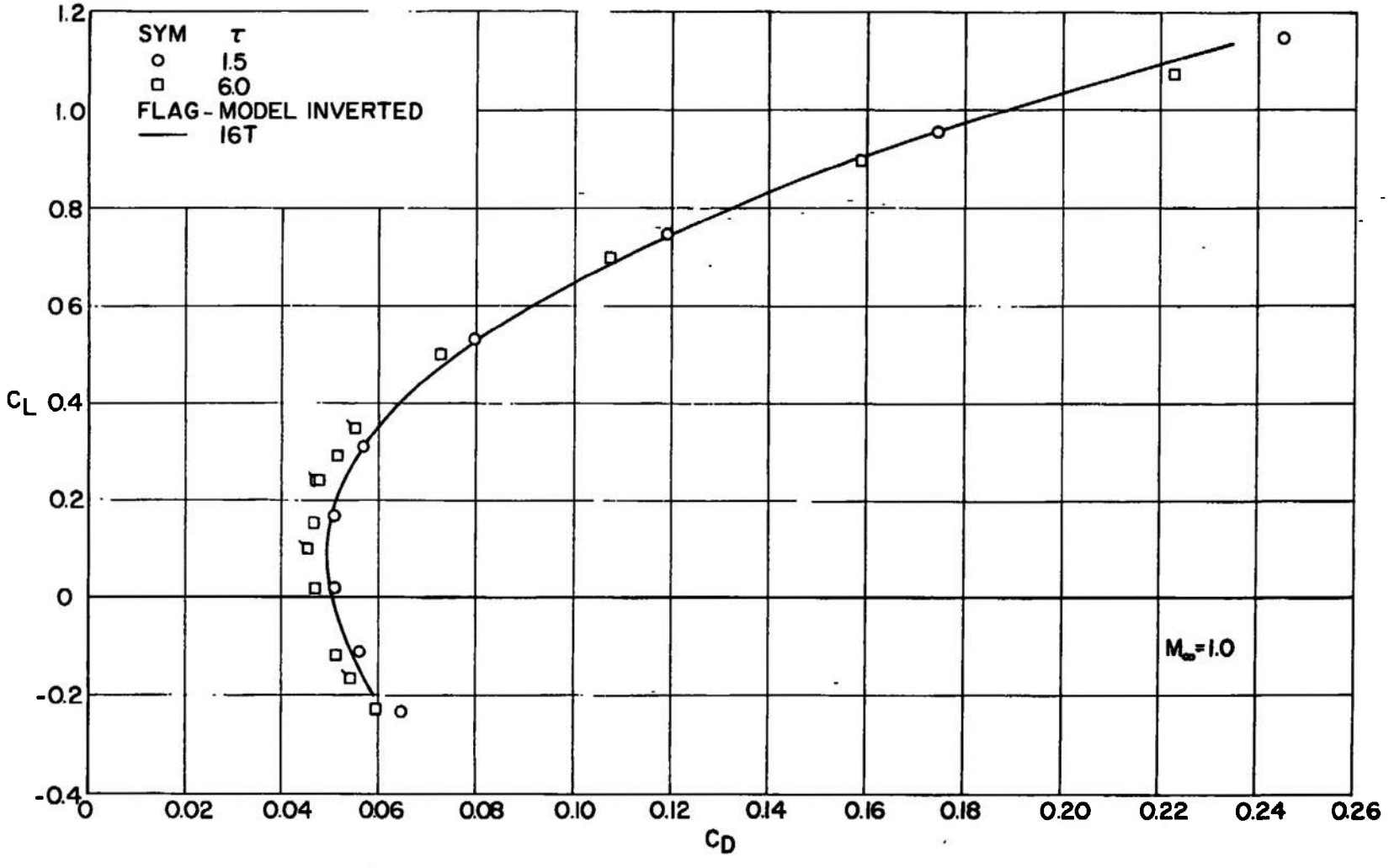

b. Drag

Fig. 12 Continued

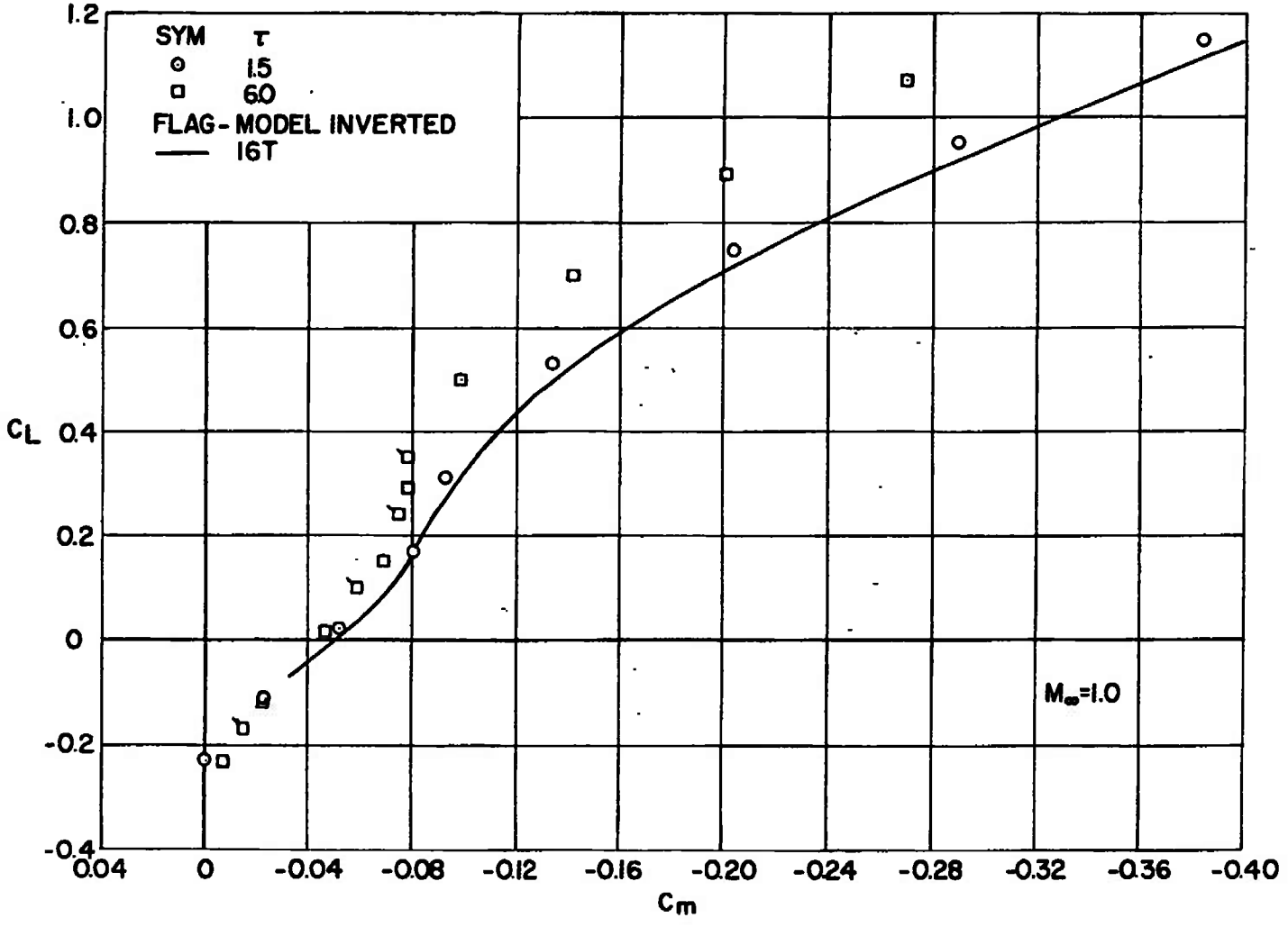

c. Pitching Moment
Fig. 12 Concluded

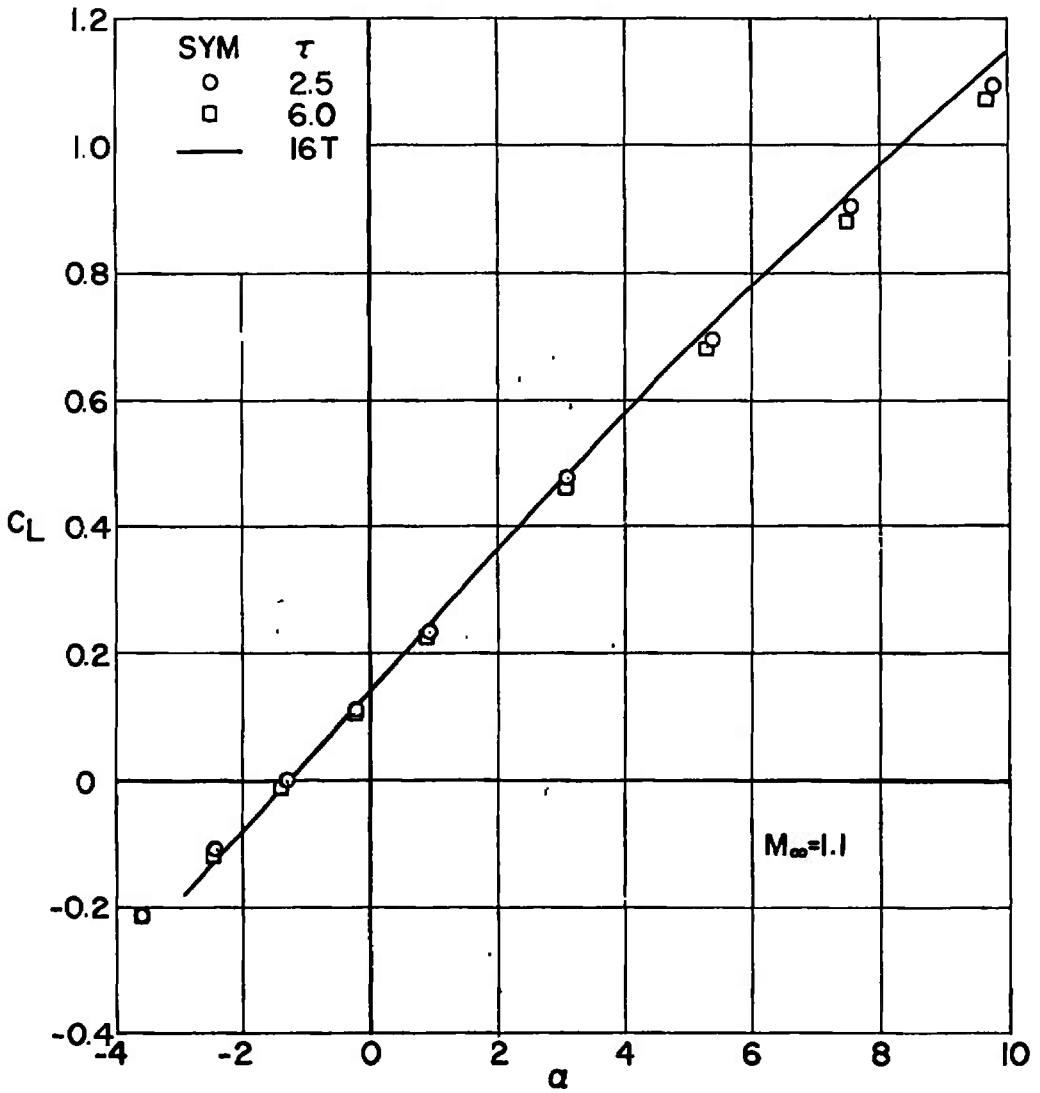

a. Lift

Fig. 13 Effect of Variable Wall Porosity in Tunnel 4T at M_∞ = 1.1

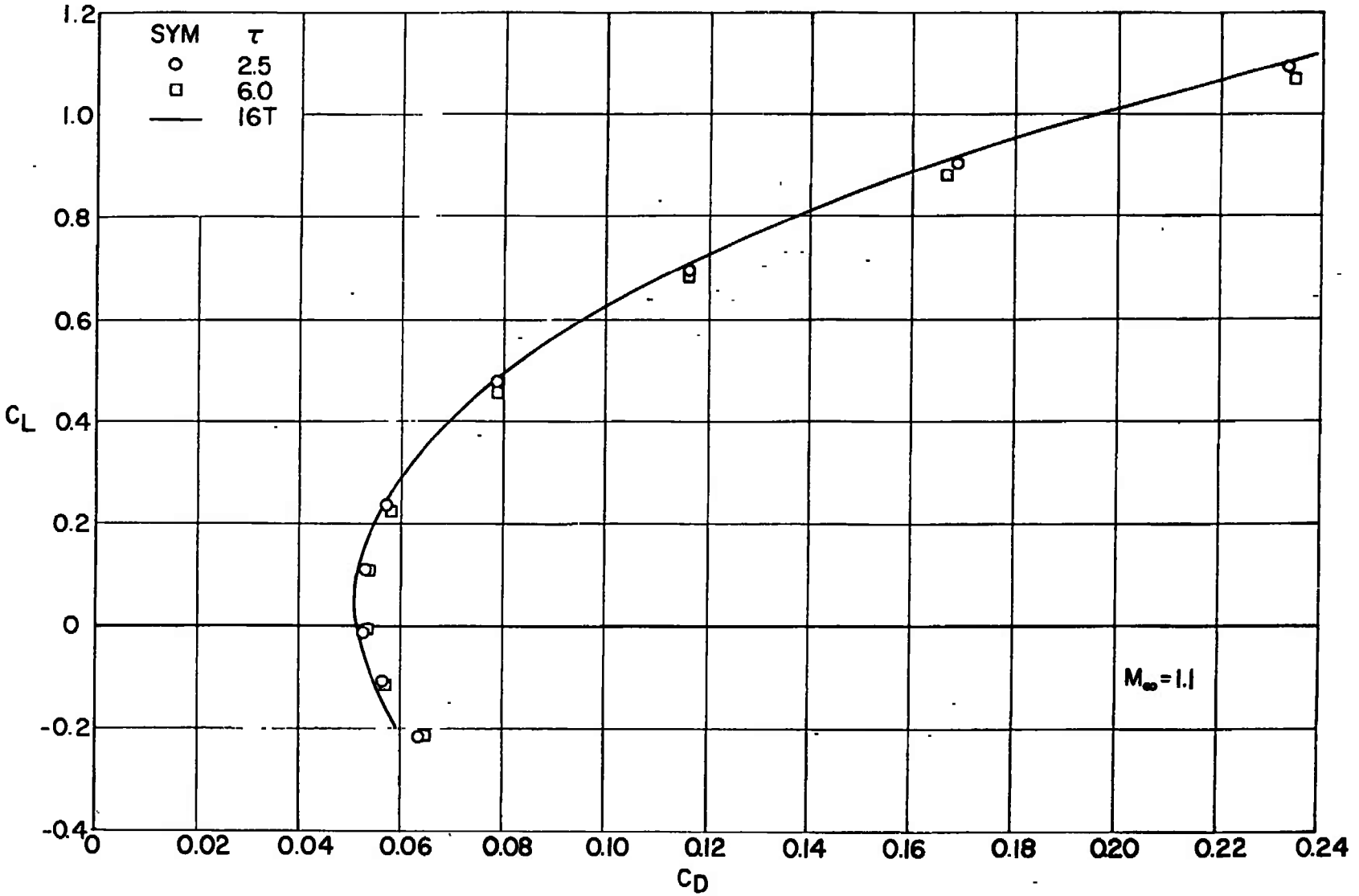

b. Drag

Fig. 13 Continued

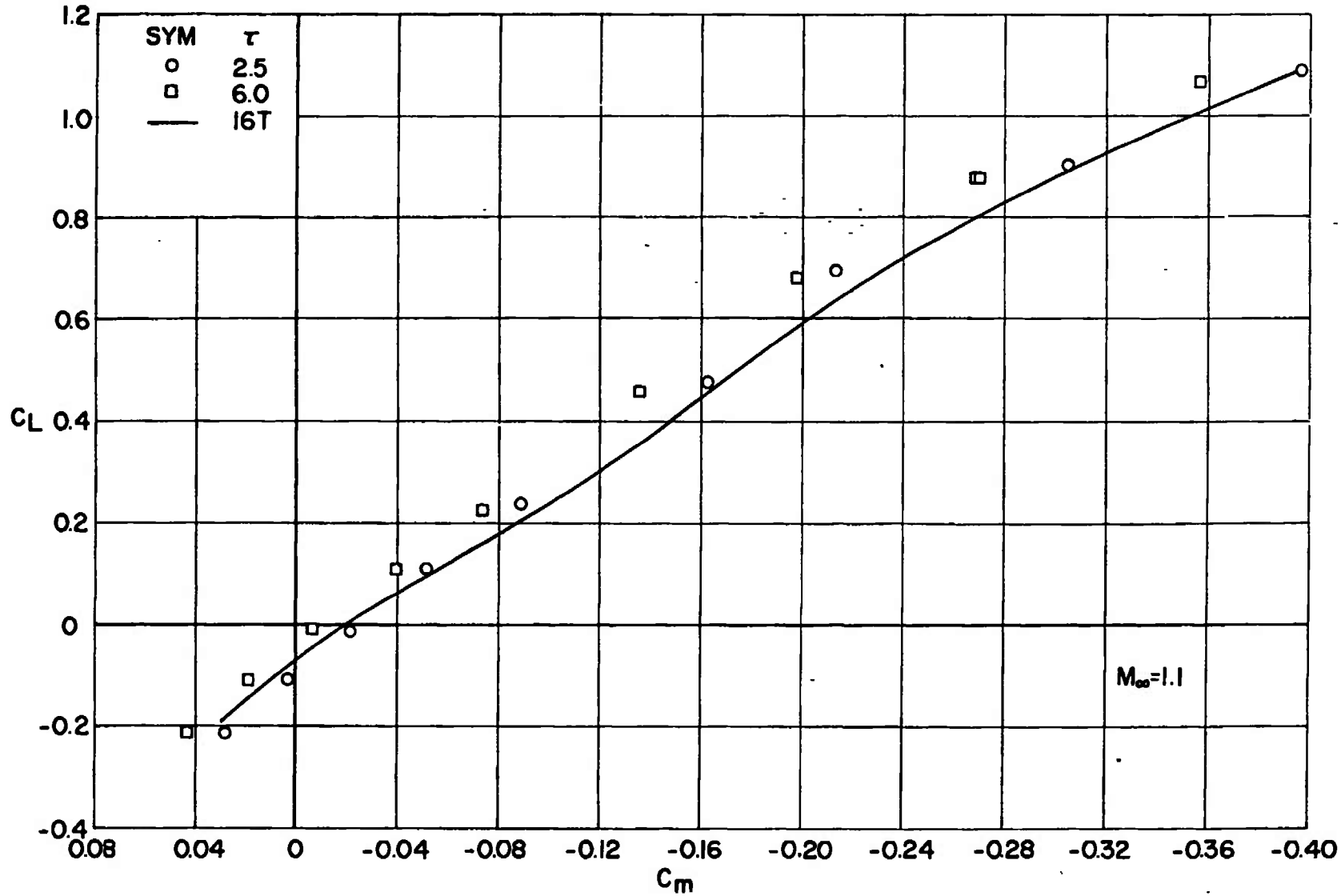

c. Pitching Moment
Fig. 13 Concluded

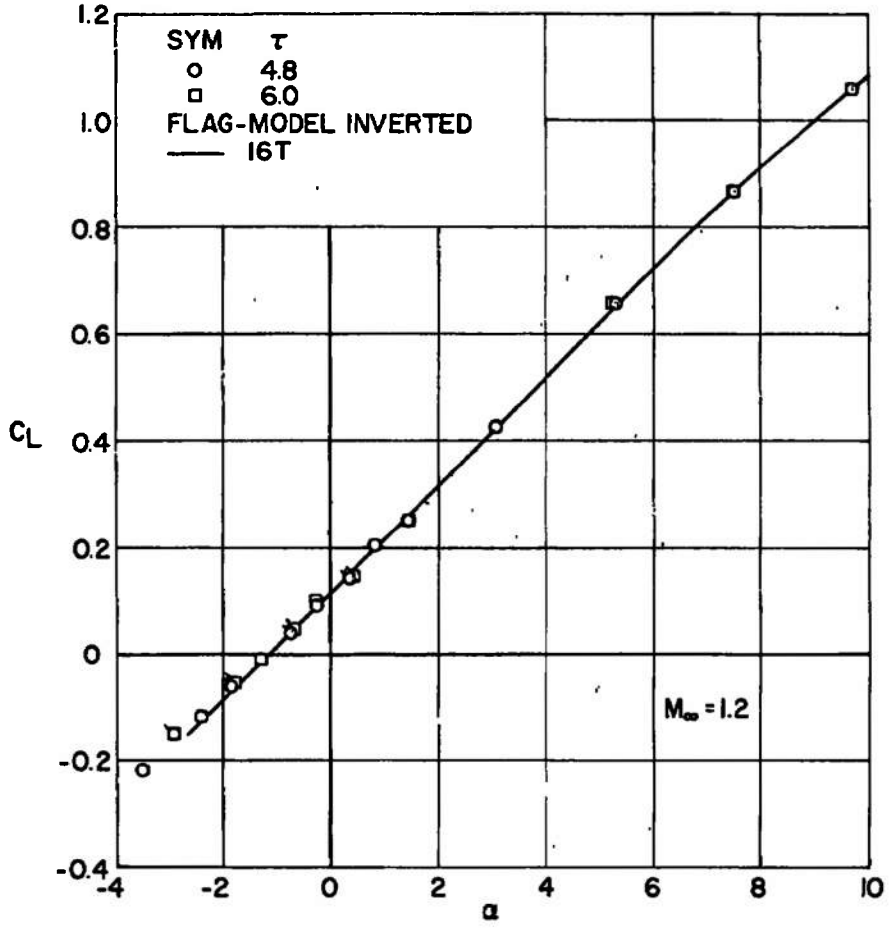

a. Lift

Fig. 14 Effect of Variable Wall Porosity in Tunnel 4T at M_∞ = 1.2

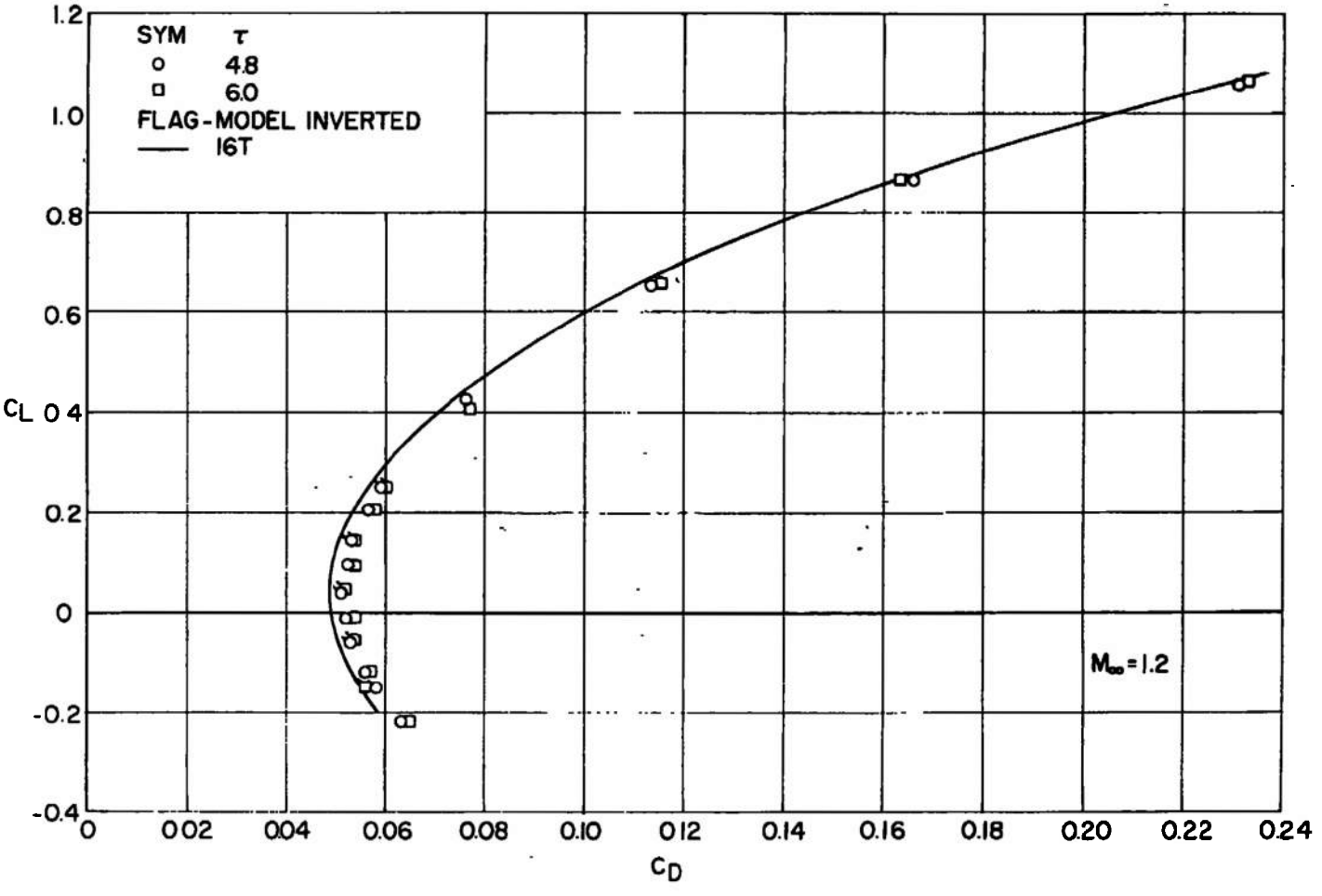

b. Drag

Fig. 14 Continued

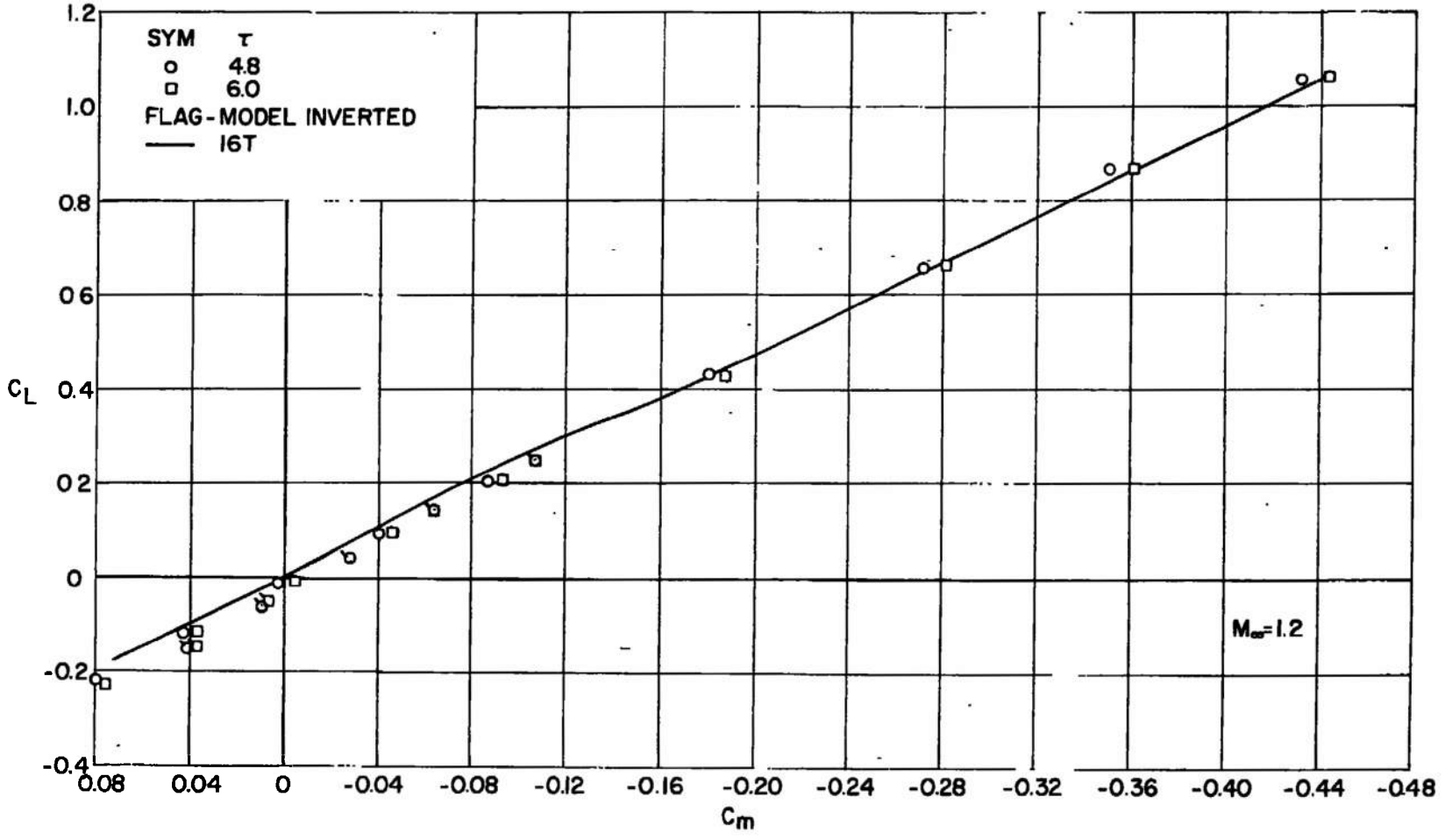

c. Pitching Moment
Fig. 14 Concluded

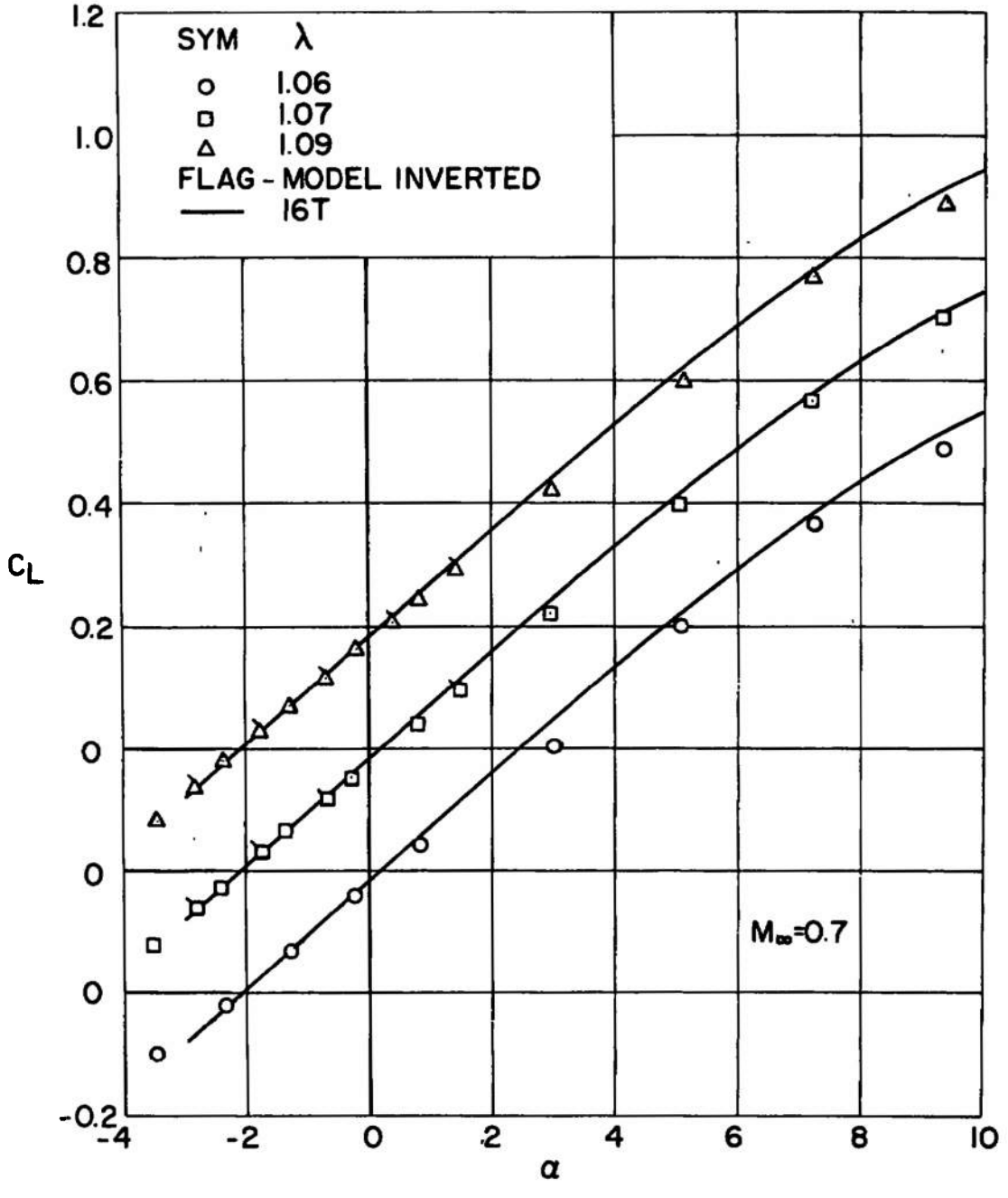

a. Lift

Fig. 15 Effect of Tunnel Pressure Ratio Variation at M_∞ = 0.7, τ = 6.0

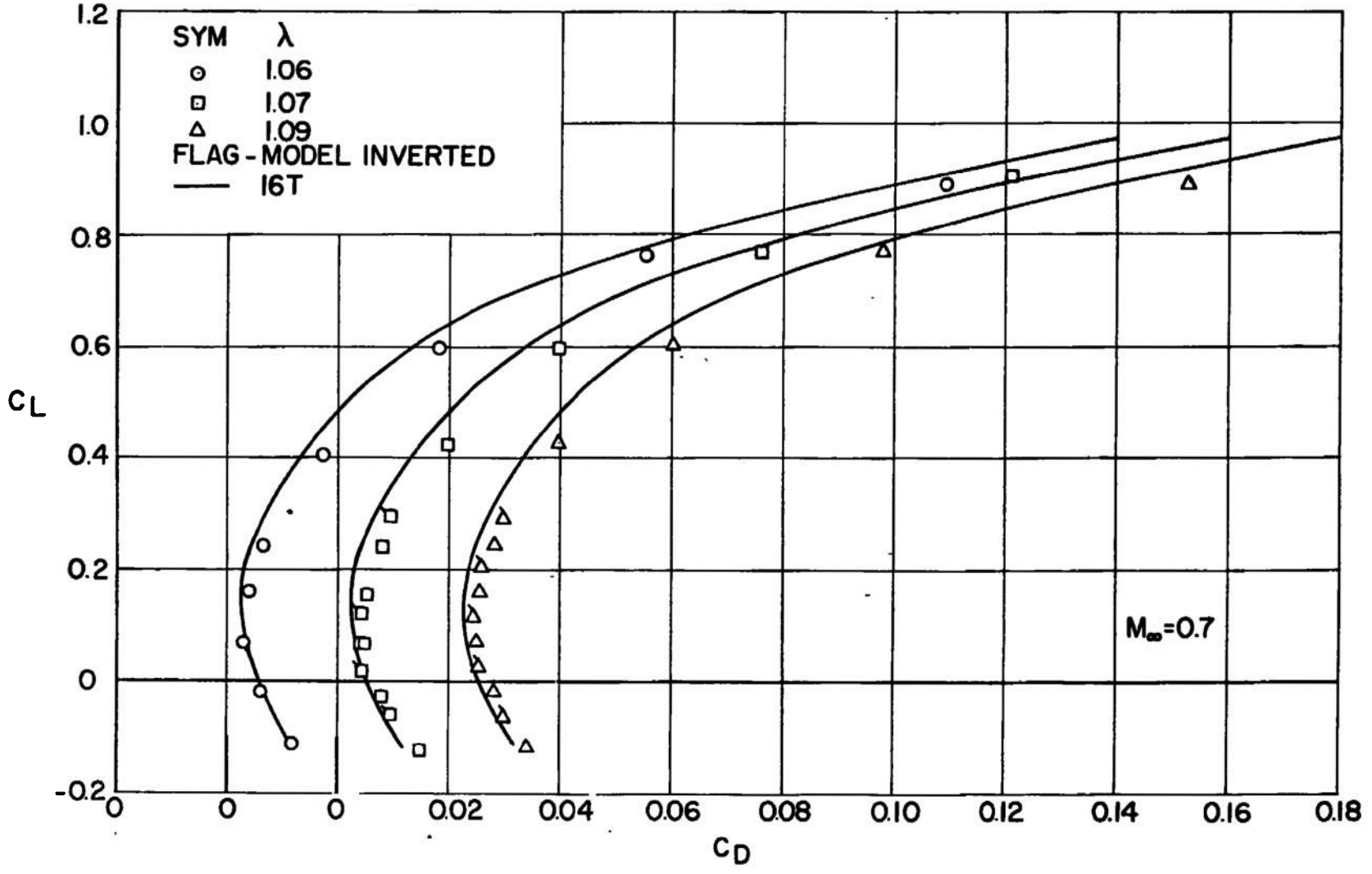

b. Drag
Fig. 15 Continued

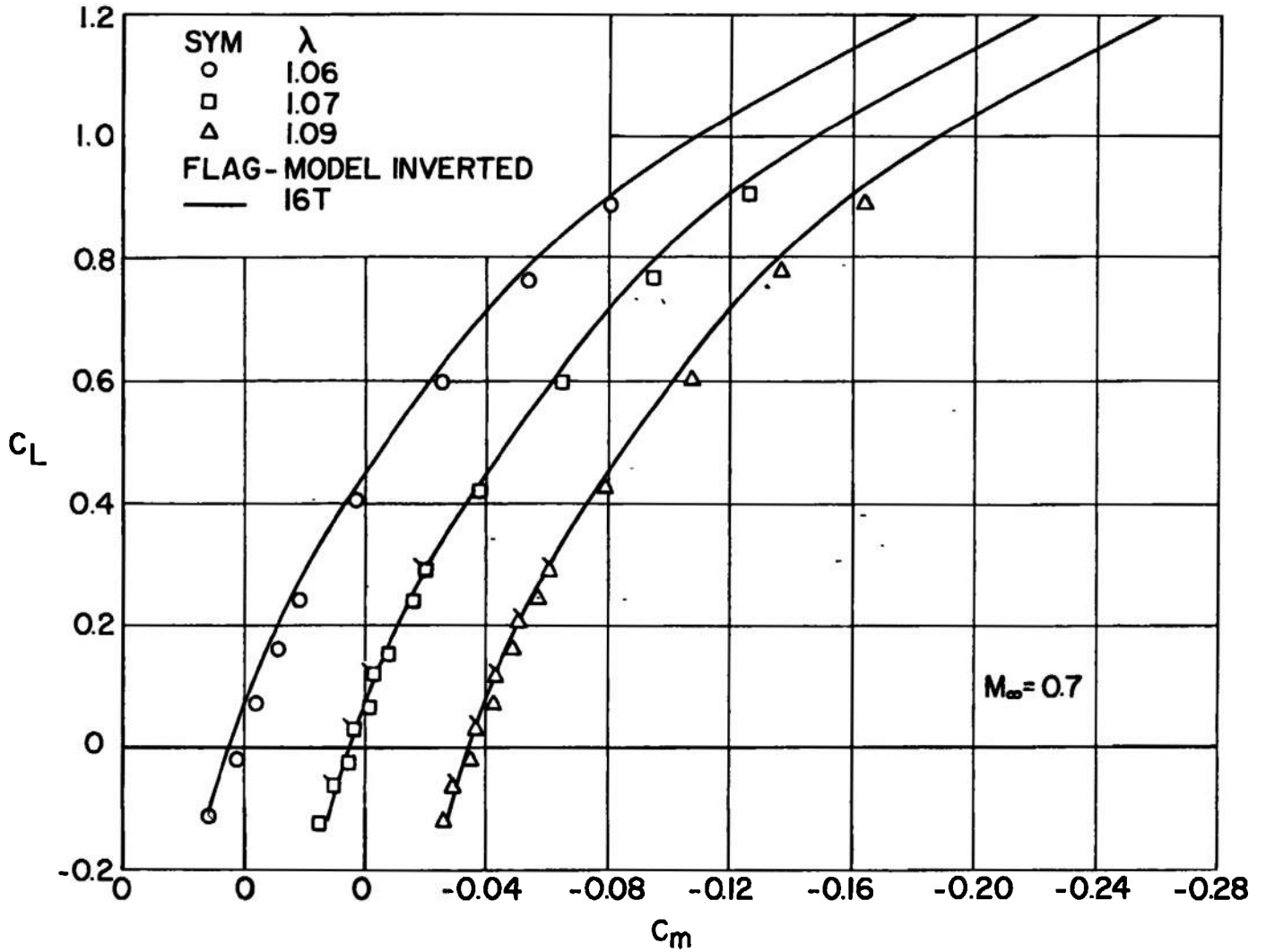

c. Pitching Moment
Fig. 15 Concluded

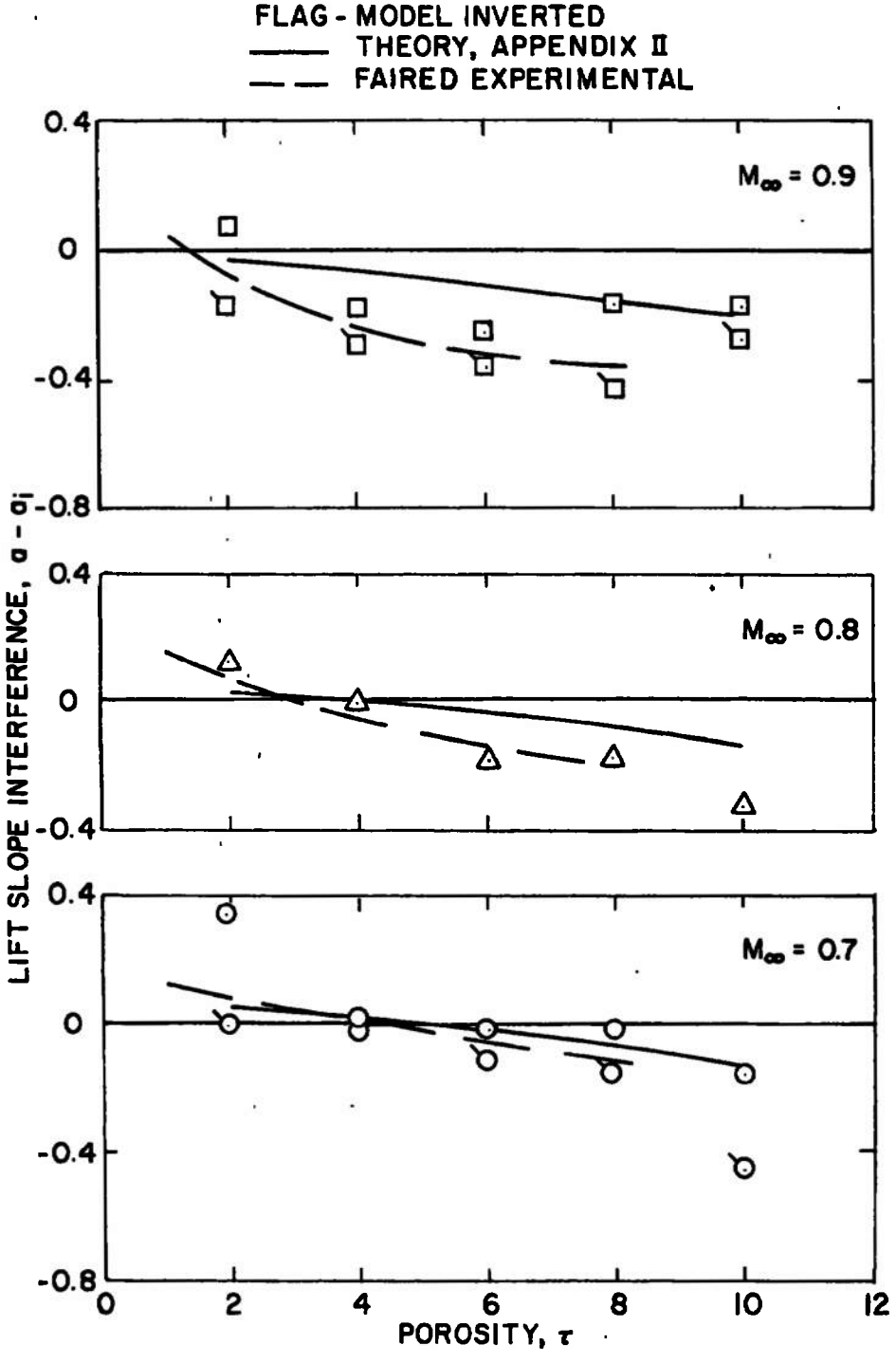

Fig. 16 Comparisons of Theoretical and Experimental Interference Effects on the Lift Curve Slope

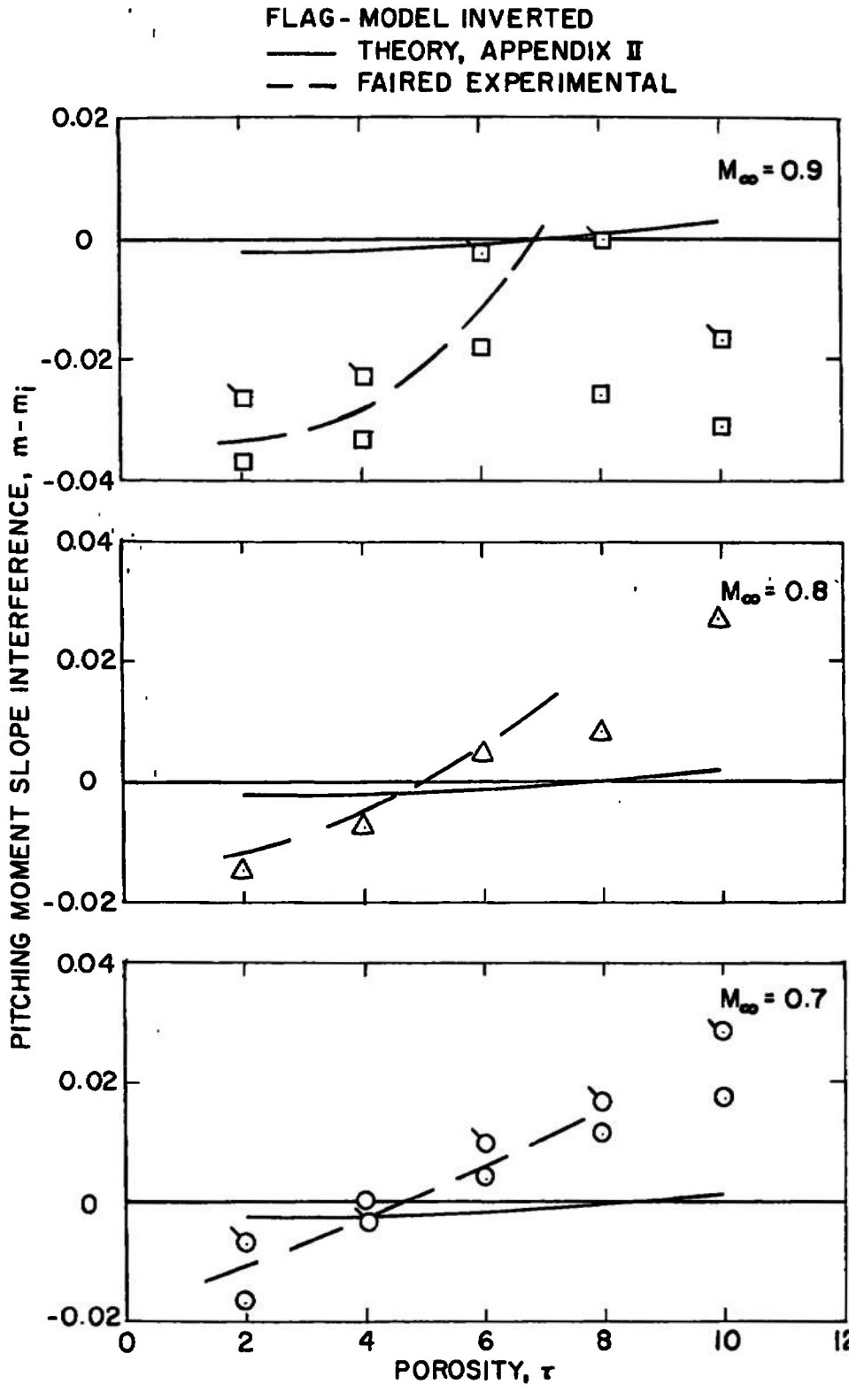

Fig. 17 Comparisons of Theoretical and Experimental Interference Effects on the Pitching-Moment Slope

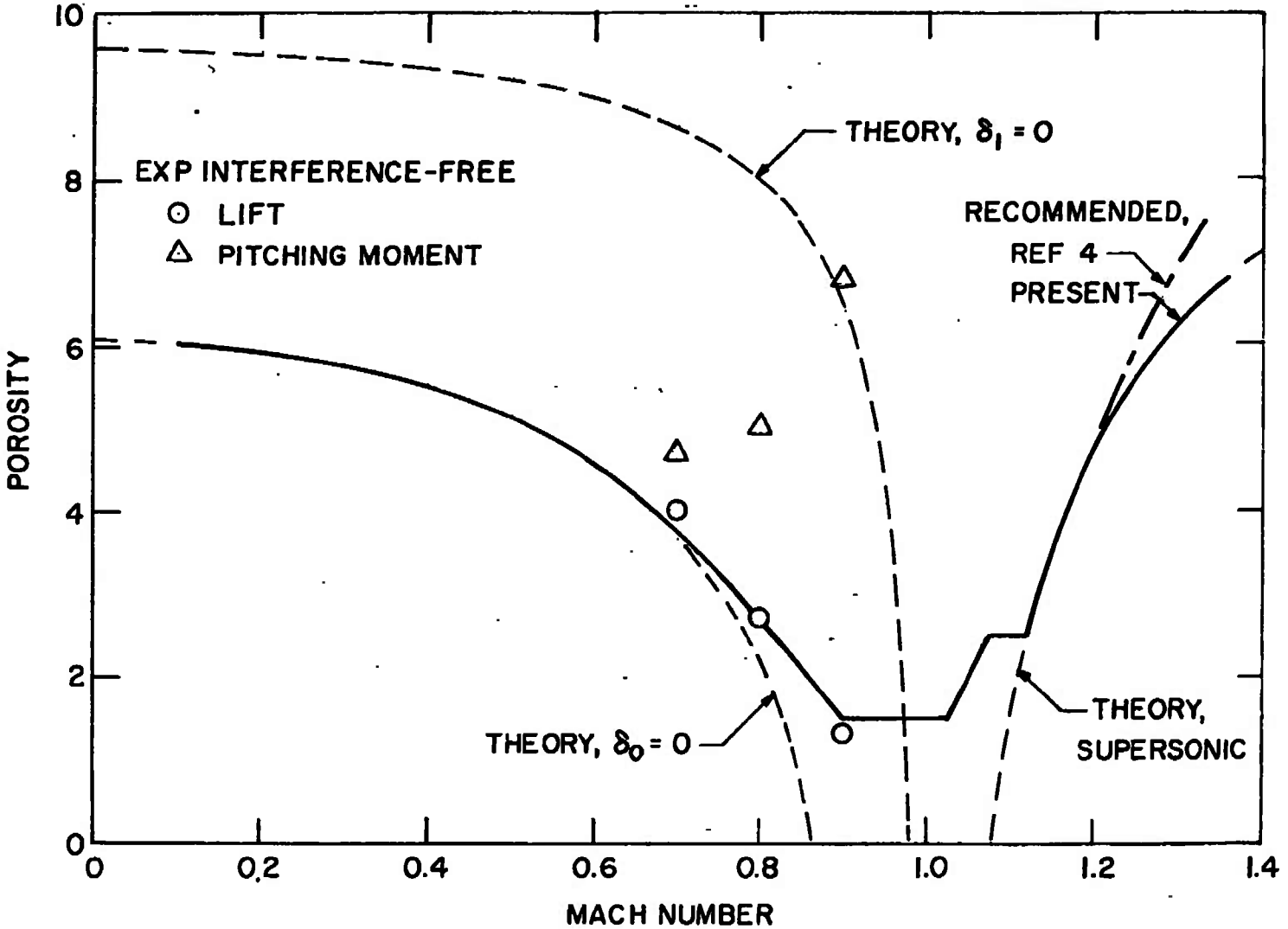

Fig. 18 Recommended Wall Porosity Schedule for Minimum Interference Effects in Tunnel 4T

APPENDIX II
THEORETICAL LIFT INTERFERENCE EFFECTS

The theoretical lift interference factors, δ_0 and δ_1, which characterize induced upwash and streamline curvature in perforated wind tunnels, are presented in Ref. 6, an extension of Ref. 7. This appendix presents the method used to transform from the theoretical parameters to the measured quantities of the present study, including previously unpublished work concerning perforated wall crossflow characteristics.

Theoretical work uses a porosity parameter, Q, defined by

$$Q = \left[1 + \frac{\beta}{2} \frac{dC_p}{d\theta}\right]^{-1} \qquad \text{(II-1)}$$

where

$$\beta = \left(1 - M_\infty{}^2\right)^{1/2}$$

C_p = wall pressure coefficient, $\dfrac{p - p_\infty}{q_\infty}$

θ = flow angle at the wall, radians
(positive for outflow from the test section)

The slope, $dC_p/d\theta$, is termed the wall crossflow characteristic, and, heretofore, was an unknown function of the wall porosity, τ. For present purposes, the functional relationship between τ and $dC_p/d\theta$ was determined as follows.

Experimental supersonic static-pressure distributions on a 20-deg cone-cylinder model in Tunnel 4T with variable wall porosity are given in Ref. 4. In general, the data are subject to wave reflection interference from the tunnel walls, there being a unique wall porosity required for wave cancellation at each Mach number. A typical example of the data is shown in Fig. II-1a, specifically for $M_\infty = 1.15$ and $\tau = 5.0$ where $\tau = 3.5$ is required to achieve interference-free data. The static-pressure distribution in conjunction with the model geometry were used as inputs to a digital computer program which utilized the method of characteristics to calculate the compatible flow field within the determinable domain. The programmed equations assumed axisymmetric, isentropic flow. Once the characteristic network was defined, interpolations for local flow properties were made at a radius which corresponded to the wall location based upon the model blockage, that is, the square

tunnel was replaced with a circular boundary of equal cross-sectional area. The calculated local pressure coefficient as a function of the local flow angle generally appeared as shown in Fig. II-1b. A least-squares second-order curve fit to the results was made, and the slope of the curve evaluated at $\theta = 0$ was taken to be the desired parameter, $dC_p/d\theta$.

The above process was repeated for each available combination of wall porosity and Mach number within the range of $1.1 < M < 1.4$, and the results are given in Fig. II-2. Within this Mach number range, the slope $dC_p/d\theta$ is sensibly independent of Mach number at a given wall porosity. Reference 8 presents data in a different format which shows the crossflow characteristics of thick-plate orifices with the approach flow perpendicular to the hole axis to be independent of the approach Mach number at low pressure differentials within the range of $0 < M < 0.6$. It is, therefore, assumed that the results shown in Fig. II-2 are valid for Tunnel 4T for all Mach numbers. For present purposes, the results are approximated by

$$\frac{dC_p}{d\theta} = 5 - \frac{5}{12}\tau \qquad \text{(II-2)}$$

As a matter of record, similar calculations using data obtained on cone-cylinder models in 1- and 16-ft transonic tunnels with 60-deg inclined-hole fixed-porosity perforated test sections show $dC_p/d\theta$ to be nominally 25 percent higher than Tunnel 4T at a given wall porosity.

For supersonic flow, small perturbation theory gives the required $dC_p/d\theta$ for wave cancellation as

$$\left[\frac{dC_p}{d\theta}\right]_{req} = \frac{2}{(M_\infty{}^2 - 1)^{1/2}} \qquad \text{(II-3)}$$

Equating (II-2) and (II-3) yields the theoretical Tunnel 4T porosity required for wave cancellation.

$$\tau = 12 - \frac{24}{5(M_\infty{}^2 - 1)^{1/2}} \qquad \text{(II-4)}$$

For subsonic flow, substituting Eq. (II-2) into Eq. (II-1) yields the desired relationship between τ and Q

$$\tau = 12 - \frac{24}{5\beta}\left(\frac{1}{Q} - 1\right) \qquad \text{(II-5)}$$

Reference 6 shows that $\delta_0 = 0$ at $Q = 0.447$ and $\delta_1 = 0$ at $Q = 0.666$. Use of these Q values in Eq. (II-5) then yields the theoretical Tunnel 4T porosities required for elimination of the two types of lift interference. The required porosities are not equal so that, in general, the lift interference will change the effective model angle of attack, given in Ref. 7 as

$$\Delta\alpha = \frac{S}{C} C_L \left[\delta_0 + \frac{\bar{c}}{8\beta h} \delta_1\right] \tag{II-6}$$

Fortunately, the first term will usually be an order of magnitude larger than the second so that the interference on lift can be practically eliminated by using the wall porosity schedule which maintains $\delta_0 = 0$.

The theoretical estimates of interference effects on the lift and pitching moment given in Figs. 16 and 17 were obtained as follows. For each combination of porosity and Mach number, the corresponding Q was evaluated from Eq. (II-5). The values of δ_0 and δ_1 were then obtained from Ref. 6 as a function of Q. Finally, the theoretical lift and pitching-moment slopes were obtained from Eq. (II-6) rewritten as, respectively

$$a = \left[\frac{1}{a_i} - \delta_0 \frac{S}{C} - \frac{\bar{c}}{8\beta h} \frac{S}{C} \delta_1\right]^{-1} \tag{II-7}$$

$$m = m_i a_i \left[\frac{1}{a} + \frac{S}{C} \delta_0 + \frac{S}{C} \left(\frac{\bar{c}}{8\beta h} + \frac{C_{m_{\alpha_t}}}{m_i a_i} \frac{\ell}{2\beta h}\right) \delta_1\right] \tag{II-8}$$

The tail effectiveness was evaluated using

$$C_{m_{\alpha_t}} = - \frac{q_t}{q_\infty} \frac{S_t}{S} \frac{\ell}{\bar{c}} \frac{dC_L}{d\alpha_t} \tag{II-9}$$

where $dC_L/d\alpha_t$ and q_t/q_∞ were obtained from Ref. 9. The estimated values of $C_{m_{\alpha_t}}$ are probably not correct, although the best available, so that the theoretical curves given in Fig. 17 are to be considered with caution. It is clear that attempts to experimentally verify the theoretical work of Refs. 6 and 7 should include direct measurements of the horizontal tail effectiveness.

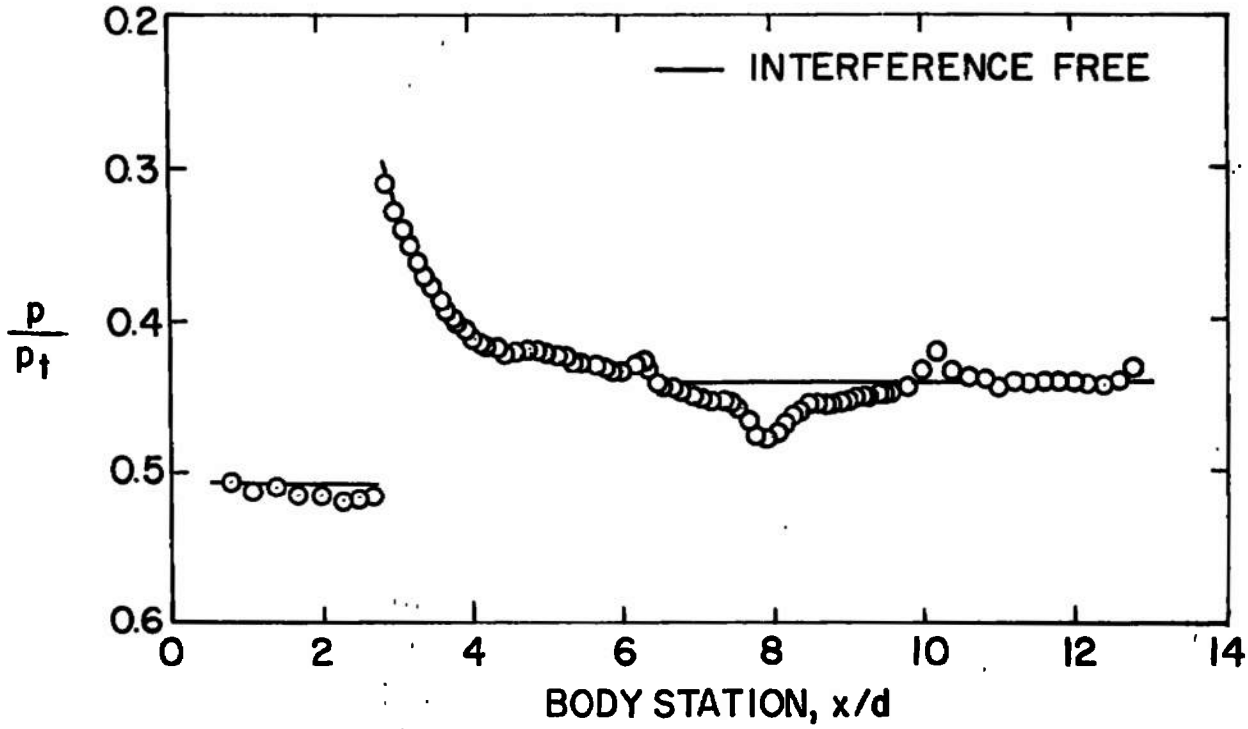

a. Pressure Distribution

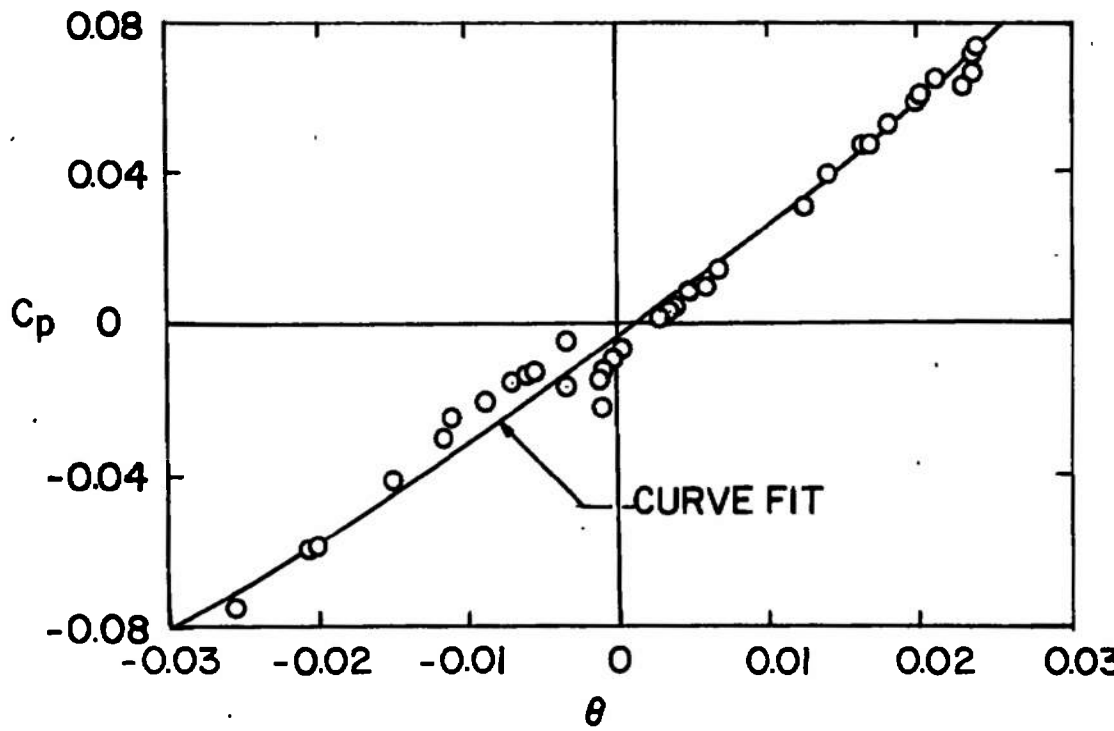

b. Crossflow Characteristic

Fig. II-1 Pressure Distribution on a Cone-Cylinder Model with the Corresponding Calculated Wall Crossflow Characteristic

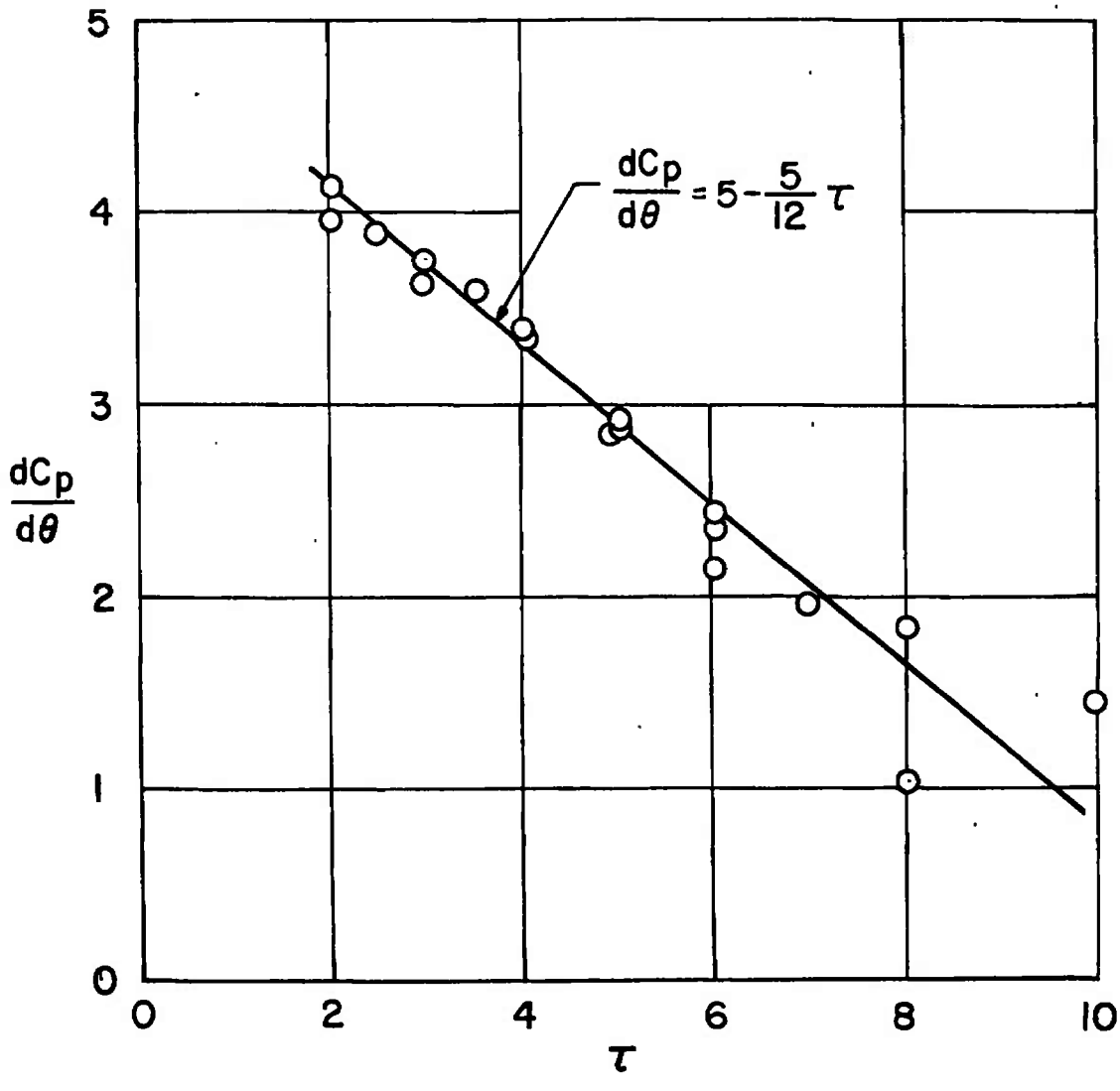

Fig. II-2 Crossflow Characteristics of the Tunnel 4T Variable Porosity Test Section Walls

UNCLASSIFIED

Security Classification

DOCUMENT CONTROL DATA - R & D

(Security classification of title, body of abstract and indexing annotation must be entered when the overall report is classified)

1. ORIGINATING ACTIVITY (Corporate author) Arnold Engineering Development Center ARO, Inc., Operating Contractor Arnold Air Force Station, Tennessee	2a. REPORT SECURITY CLASSIFICATION UNCLASSIFIED 2b. GROUP N/A

3. REPORT TITLE

EVALUATION OF INTERFERENCE EFFECTS ON A LIFTING MODEL IN THE AEDC-PWT 4-FT TRANSONIC TUNNEL

4. DESCRIPTIVE NOTES (Type of report and inclusive dates)

September 6, 1969 - Final Report

5. AUTHOR(S) (First name, middle initial, last name)

J. L. Jacocks, ARO, Inc.

6. REPORT DATE April 1970	7a. TOTAL NO. OF PAGES 63	7b. NO. OF REFS 9
8a. CONTRACT OR GRANT NO. F40600-69-C-0001 b. PROJECT NO. c. Program Element 65401F/06RB d.	9a. ORIGINATOR'S REPORT NUMBER(S) AEDC-TR-70-72 9b. OTHER REPORT NO(S) (Any other numbers that may be assigned this report) N/A	

10. DISTRIBUTION STATEMENT This document is subject to special export controls and each transmittal to foreign governments or foreign nationals may be made only with prior approval of Arnold Engineering Development Center (AETS), Arnold Air Force Station, Tennessee 37389.

11. SUPPLEMENTARY NOTES Available in DDC	12. SPONSORING MILITARY ACTIVITY Arnold Engineering Development Center, Air Force Systems Command Arnold AF Station, Tennessee 37389

13. ABSTRACT

Tests were conducted in the AEDC Aerodynamic Wind Tunnel (4T) to evaluate subsonic and supersonic wall interference effects and general data quality using a modified F-111A aircraft model of 0.6-percent blockage. The tunnel is equipped with inclined-hole, variable porosity test section walls. Comparisons of the data obtained in Tunnel 4T with data obtained in the Propulsion Wind Tunnel (16T) using the same model, balance, and sting show that practically interference-free data can be obtained in Tunnel 4T throughout the Mach number range from 0.7 to 1.2 utilizing variable porosity. At other than the optimum wall porosities, experimental subsonic lift interference effects are generally larger than theoretical predictions, although theory and experiment are in qualitative agreement.

This document is subject to special export controls and each transmittal to foreign governments or foreign nationals may be made only with prior approval of Arnold Engineering Center (AETS), Arnold Air Force Station, Tennessee 37389.

DD FORM 1 NOV 68 1473

UNCLASSIFIED

Security Classification

14. KEY WORDS	LINK A ROLE	LINK A WT	LINK B ROLE	LINK B WT	LINK C ROLE	LINK C WT
F-111A aircraft						
transonic wind tunnels						
test facilities						
design						
quality assurance						
shock wave interference						
subsonic wind tunnels						

1. Airplanes -- F-111A
2. Models -- Interference
3. Wind tunnel models - "
4. Wind tunnels " "
5. Tests " "
6. " " " -- Plan
7. Transonic " " -
8. " " " -- Subsonic

17-3